HHS Public Access

Author manuscript

Cell Rep. Author manuscript; available in PMC 2024 September 07.

Published in final edited form as:

Cell Rep. 2024 May 28; 43(5): 114119. doi:10.1016/j.celrep.2024.114119.

A p85 isoform switch enhances PI3K activation on endosomes by a MAP4- and PI3P-dependent mechanism

Narendra Thapa[1], **Mo Chen**[1], **Vincent L. Cryns**[2], **Richard Anderson**[1,3,*]

[1]School of Medicine and Public Health, University of Wisconsin-Madison, 1111 Highland Avenue, Madison, WI 53705, USA

[2]Department of Medicine, School of Medicine and Public Health, University of Wisconsin-Madison, 1111 Highland Avenue, Madison, WI 53705, USA

[3]Lead contact

SUMMARY

Phosphatidylinositol 3-kinase α (PI3Kα) is a heterodimer of p110α catalytic and p85 adaptor subunits that is activated by agonist-stimulated receptor tyrosine kinases. Although p85α recruits p110α to activated receptors on membranes, p85α loss, which occurs commonly in cancer, paradoxically promotes agonist-stimulated PI3K/Akt signaling. p110α localizes to microtubules via microtubule-associated protein 4 (MAP4), facilitating its interaction with activated receptor kinases on endosomes to initiate PI3K/Akt signaling. Here, we demonstrate that in response to agonist stimulation and p85α knockdown, the residual p110α, coupled predominantly to p85β, exhibits enhanced recruitment with receptor tyrosine kinases to endosomes. Moreover, the p110α C2 domain binds PI3-phosphate, and this interaction is also required to recruit p110α to endosomes and for PI3K/Akt signaling. Stable knockdown of p85α, which mimics the reduced p85α levels observed in cancer, enhances cell growth and tumorsphere formation, and these effects are abrogated by MAP4 or p85β knockdown, underscoring their role in the tumor-promoting activity of p85α loss.

In brief

In this work, Thapa et al. define a mechanism by which p85α loss, which occurs in cancer, leads to the coupling of p110α with p85β (isoform switch), which promotes enhanced association with receptors and p110α C2 domain-dependent targeting to endosomes regulated by PI3P and MAP4, culminating in paradoxically increased agonist-stimulated PI3K/Akt signaling.

Graphical Abstract

*Correspondence: raanders@wisc.edu.

AUTHOR CONTRIBUTIONS

N.T., M.C., V.L.C., and R.A. designed and discussed experiments. N.T. and M.C. performed experiments. N.T., M.C., V.L.C., and R.A. discussed and wrote the manuscript.

DECLARATION OF INTERESTS

The authors declare no competing interests.

SUPPLEMENTAL INFORMATION

Supplemental information can be found online at https://doi.org/10.1016/j.celrep.2024.114119.

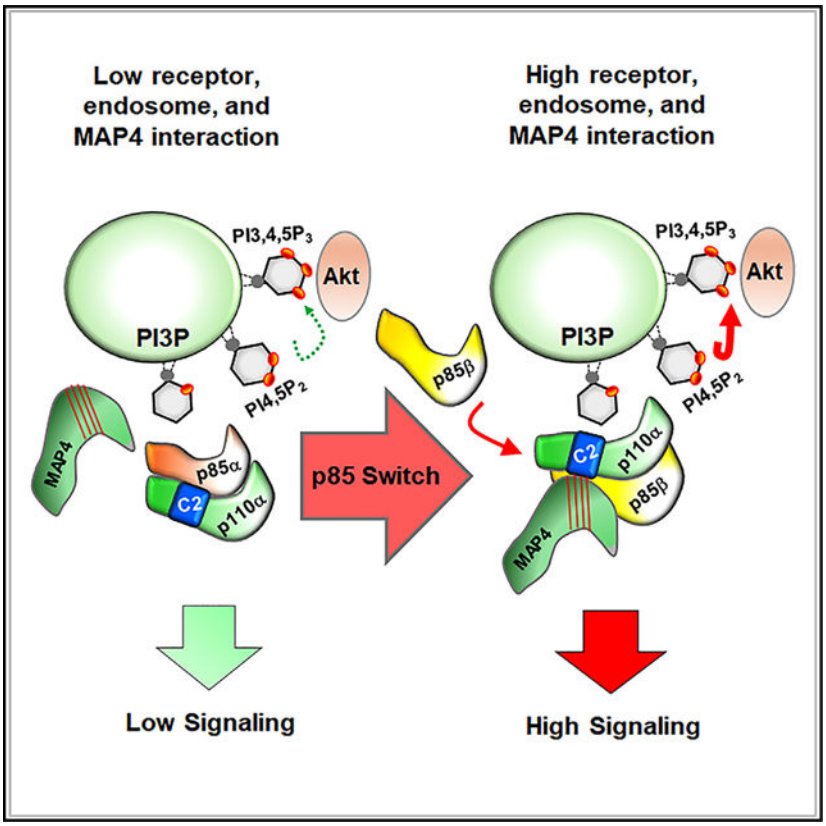

INTRODUCTION

The class IA phosphatidylinositol (PI) 3-kinase (PI3K) responsible for activating PI3K/Akt signaling downstream of agonist-stimulated receptor tyrosine kinases is a heterodimer composed of adaptor (p85α, p55α, p50α, p85β, and p55γ) and catalytic (p110α, p110β, and p110δ) subunits.[1,2] Src homology 2 (SH2) domain-mediated recruitment of the p85 adaptor subunit to phosphorylated YXXM motifs on activated receptor tyrosine kinases liberates the intermolecular constraints imposed on the p110 catalytic subunit, allowing it to the interact with the membrane surface to catalyze PI 4,5-bisphosphate ($PI4,5P_2$) phosphorylation, generating $PI3,4,5P_3$.[3] $PI3,4,5P_3$, in turn, recruits Akt and the Akt-activating kinases PDK1 and mTORC2 (Sin1 subunit) via their pleckstrin homology domains to activate Akt by catalyzing Akt phosphorylation on T^{308} and S^{473}, respectively.[4]

Despite a role for p85 in recruiting/activating the p110α catalytic subunit, heterozygous deletion of the p85α gene in mice paradoxically upregulates PI3K/Akt signaling downstream of the insulin receptor (IR).[5–7] Similarly, liver-specific deletion of the p85α gene leads to increased PI3K/Akt signaling and hepatocellular carcinoma.[8] Moreover, p85α mRNA and protein levels are often downregulated in breast cancer, bladder cancer, cancer-associated fibroblasts, and other tumor types, implicating p85α as a tumor suppressor.[8–11] Several studies have demonstrated decreased p85α expression but increased p85β expression in cancer, suggesting opposing functions for the p85 isoforms.[12–14] Although several potential explanations for the paradoxical increase in agonist-stimulated PI3K/Akt

signaling in response to p85α loss[1,9,14] have been postulated, the underlying mechanisms remain largely unknown. Given the frequent loss of p85α expression in cancer and its tumor-suppressive function,[8,9] the elucidation of these mechanisms could lead to a better understanding of therapeutic targets for cancer.[8]

In PI3Kα heterodimers, the membrane recruitment of the p110α catalytic subunit is critical, as induced membrane targeting of p110α via myristoylation drives constitutive PI3K/Akt signaling and is highly oncogenic.[15] Although the p85 adaptor subunits recruit p110α to activated receptor tyrosine kinases at the plasma membrane or endomembrane, multiple domains of p110α, including the Ras-binding domain, the C2 domain, and the catalytic domain can directly or indirectly recruit p110 to the membrane.[3,16,17] Specifically, the C2 domain is a well-defined membrane-binding module present in the catalytic subunit of all PI3Ks (class I, II, and III) and many other proteins such as PTEN and PKC.[3,18,19] However, the precise role of the PI3Kα C2 domain in membrane targeting in response to agonist-stimulated PI3K/Akt signaling remains poorly understood.

Previously, we introduced the concept of IQGAP1 and microtubule-associated protein 4 (MAP4) scaffolding of PI3Kα in the regulation of the agonist-stimulated PI3K/Akt signaling pathway.[20,21] Specifically, PI3Kα is recruited by a MAP4-dependent mechanism to the endosomal compartment, where it binds activated receptor tyrosine kinases to initiate PI3K-Akt signaling,[21] and IQGAP1 is a component of this complex.[20,22] In the present study, we discovered that p85α knockdown (KD) augments agonist-stimulated PI3K/Akt signaling predominantly at endosomal membranes. Although the expression level of p110α is substantially reduced upon p85α KD, the residual p110α, coupled largely to p85β, localizes along microtubules by binding MAP4, resulting in its recruitment to endosomal membranes and association with activated epidermal growth factor receptor (EGFR). Several basic amino acid residues in the C2 domain of p110α mediate its interaction with the endosomal phosphoinositide PI3-phosphate (PI3P), a key step in recruiting p110α to endomembranes and activating PI3K/Akt signaling. Stable KD of p85α in cancer cells enhances cell growth and tumorsphere formation by a MAP4/p85β/PI3K-dependent mechanism, underscoring the pathogenic relevance of our findings for cancer. Overall, these results provide a comprehensive mechanism for the seemingly paradoxical enhanced activation of agonist-stimulated PI3K/Akt signaling in the setting of p85α loss and highlight its role in tumor growth.

RESULTS

p85α adaptor subunit KD promotes Akt activation downstream of multiple receptor tyrosine kinases

We first examined the effect of p85α KD on agonist-stimulated Akt activation using small interfering RNAs (siRNAs) that target all the transcriptional variants of p85α (p85α, p55α, and p50α). KD of p85α enhanced Akt activation by multiple agonists as determined by western blot (WB) of pAkt levels (Figures 1A–1D). Moreover, three individual siRNAs targeting p85α similarly promoted EGF-stimulated Akt activation (Figure 1E). p85α KD promoted EGF-stimulated Akt activation in multiple cell lines (Figures S1A–S1C). We recapitulated the enhanced activation of Akt through stable KD of p85α using a lentiviral

shRNA system in MDA-MB-321 and A431 cells (Figures S1D and S1E). However, the enhanced agonist-stimulated activation of PDK1 and mTOR in response to p85α KD was observed only in A431 cells, as the basal levels of phosphorylated PDK1 and mTOR were high in MDA-MB-231 cells. Collectively, these results indicate that p85α KD augments PI3K/Akt signaling downstream of multiple receptor tyrosine kinases.[5,6]

The p85 adaptor and p110 catalytic subunit are present in 1:1 stoichiometry in the PI3K holoenzyme.[23,24] However, some studies indicate that the p85 adaptor subunit is more abundant than the p110 catalytic subunit (10%–30% more depending on cell types and tissues). Moreover, the free p85α adaptor subunit has been postulated to compete with PI3Kα heterodimers for binding to activated receptor tyrosine kinases, resulting in impaired PI3K/Akt signaling.[1,24] To investigate whether this mechanism contributes to enhanced Akt activation in response to p85α KD, we first performed a dose-response experiment using increasing concentrations of p85α siRNAs. The degree of p85α KD correlated inversely with EGF-stimulated pAkt levels, with the most robust activation noted when p85α KD was >70% (Figure 1F). We next examined the effect of ectopically overexpressing p85α on EGF-stimulated PI3K/Akt signaling. Robust overexpression of p85α had no effect on EGF-stimulated Akt activation (Figure 1G) despite efficient co-immunoprecipitation (coIP) of the endogenous p110α subunit with FLAG-tagged p85α (Figure 1H). These results argue against the concept that excess p85α adaptor subunits compete with the PI3Kα heterodimers for activated receptor tyrosine kinases in these cellular models.

p85α binds PTEN, and increased PI3K/Akt signaling upon p85α loss has been attributed to compromised PTEN recruitment to membranes to antagonize PI3K/Akt signaling.[25] To investigate this possibility, we examined the effects of p85α KD on EGF-stimulated Akt activation in PTEN-null PC-3 prostate cancer cells. p85α KD enhanced EGF-stimulated Akt activation in these PTEN-null cells (Figure 1H). Furthermore, combined KD of p85α and PTEN resulted in more robust Akt activation under basal and EGF-stimulated conditions than individual KD of p85α or PTEN (Figures 1J and 1K). Taken together, these findings demonstrate that the enhanced agonist-stimulated activation of Akt in response to p85α loss is PTEN independent in these cellular models.

PI3,4,5P_3 generation and Akt activation induced by agonist stimulation and p85α KD occur at the endomembrane

Although the prevailing dogma is that agonist-stimulated PI3,4,5P_3 generation and Akt activation occur exclusively at the plasma membrane,[3,26] we recently demonstrated that PI3,4,5P_3 generation and Akt activation downstream of activated receptor tyrosine kinases occur predominantly in internal membrane compartments.[21] In response to agonist stimulation, PI3Kα distributes along microtubules, and receptor tyrosine kinases are rapidly internalized and activated on endosomes to initiate agonist-stimulated PI3,4,5P_3 generation and Akt activation in the endomembranes.[21,27–29] We examined the expression and phosphorylation levels of EGFR, IR, and Akt following agonist stimulation in a time course using control vs. p85α short hairpin RNA (shRNA) cells. EGFR, IR, and Akt were robustly phosphorylated within 5 min (Figures 2A and 2B). After 30–60 min, the activation of both receptors and Akt decreased. Notably, the kinetics and activation levels

of EGFR and IR were comparable throughout the time course in control vs. p85α shRNA cells, but pAkt levels were consistently greater in p85α shRNA cells compared to controls cells at each time point. Moreover, the internalized EGFR co-localized with the endosomal marker early endosome antigen 1 (EEA1) following EGF stimulation (Figures 2C and 2D) to a comparable degree in control vs. p85α shRNA cells. As internalized EGFR in early endosomes progresses to late endosomes/lysosomes, the number of EGFR-EEA1-positive puncta decreased in alignment with decreased phosphorylation of receptors and decreased Akt activation. Congruent with our WB results (Figure 1), EGF stimulation and p85α KD each augmented pAkt and PI3,4,5P_3 levels as determined by immunofluorescence (IF) (Figures S2A and S2B). Consistent with this result, p85α KD increased the number of EEA1- and transferrin receptor (TFR)-positive endosomes that co-localized with activated Akt and PI3,4,5P_3 in response to EGF stimulation (Figures 2E, 2F, S2C, and S2D). Next, we isolated plasma membrane- and endosomal membrane-enriched fractions as described previously[21] and observed that p85α KD and EGF stimulation each activated Akt predominantly in the EEA1-enriched endosomal fraction (Figure 2G). Similarly, the analysis of activated Akt in different subcellular fractions (plasma membrane, cytosol, endosome, and nuclear fractions) of another cell line (A431) validated the spatial enrichment of activated Akt in the endosomal fraction and its enhanced activation in response to p85α KD (Figure 2H). These data indicate that the increased agonist-stimulated PI3,4,5P_3 and pAkt levels in response to p85α KD localize largely to the endosomal membrane, aligning with our previous findings.[21]

Residual p110α catalytic subunit is responsible for increased agonist-stimulated Akt activation in response to p85α KD

Among class IA PI3Ks, PI3Kα and PI3Kβ are ubiquitously expressed enzymes in non-hematopoietic cells, and PI3Kδ is expressed in hematopoietic cells.[2] As the p85 adaptor subunit stabilizes p110 catalytic subunits, we examined the expression level of p110α and p110β catalytic subunits upon p85α or p85β KD. p85α KD (more than 90%) resulted in an ~60% decrease in p110α levels but only an ~25% reduction in p110β levels (Figure 3A). p85β KD resulted in an ~20% decrease in p110α levels and an ~10% reduction in p110β levels. To examine the contribution of p110α and p110β catalytic subunits to Akt activation in response to p85α KD and agonist stimulation, we used siRNAs to knock down p85α and p110α or p110β. KD of p110α, but not p110β, inhibited EGF-stimulated Akt activation upon EGF stimulation (Figure 3B), indicating that the residual p110α catalytic subunit is responsible for activating PI3K/Akt signaling in response to p85α KD, consistent with PI3Kα inhibitor blockade of PI3K/Akt signaling in response to p85α KD.[9] Furthermore, overexpression of p110α augmented EGF-stimulated Akt activation in response to p85α KD (Figure 3C), providing additional evidence for the functional role of p110α in these events.

Next, we undertook a semiquantitative mass spectrometry approach to analyze the p110α catalytic subunit-associated adaptor subunits in response to p85α KD. The analysis of spectral counts of proteins that coIPed with p110α indicated that p85α and p85β constituted ~40% and ~57% of p85 adaptor subunits, respectively (together ~97%), that associated with p110α in cells treated with non-silencing control (siCon) siRNAs (Figure 3D). In response to p85α KD, p85β association with p110α increased from ~57% to ~72%, with ~14%

of p110α not associated with any p85 adaptor subunits (Figure 3D). We did not detect p55γ or its association with p110α in the cells examined. These results were validated by coIP experiments, which revealed increased p85β association with residual p110α in response to p85α KD (Figure 3E). In alignment with the tumor-promoting role of p85β, p85β KD dramatically impaired EGF-stimulated Akt activation (Figure 3F). However, KD of both p85α and p85β adaptor proteins virtually abolished p110α expression and EGF-stimulated Akt activation (Figure 3G). These results indicate that p110α retains competency for receptor tyrosine kinases in response to p85α KD, likely through increased coupling with p85β.

Residual p110α localizes to microtubules, integrates into endosomes, and associates with receptor kinases in response to p85α KD

We recently demonstrated that PI3Kα localizes to microtubules via a direct interaction of p110α with MAP4.[21] MAP4 serves as a scaffolding molecule to recruit PI3Kα vesicles along microtubules, facilitating its incorporation into endosomes containing active receptors.[21] Consistent with these results, residual p110α localized along microtubules following p85α KD (Figure S3A) and co-localized with MAP4 in a pattern indistinguishable from cells treated with siCon (Figure 4A, top). p85α KD enhanced the interaction of residual p110α with MAP4 (Figures 4A, bottom, S3B, and S3C). Furthermore, agonist stimulation enhanced the association of residual p110α with MAP4 in p85α shRNA cells (Figure 4B). Following p85α KD, the residual p110α exhibited enhanced co-localization with the endosomal markers EEA1 and TFR in response to EGF stimulation (Figures 4C and S4A–S4C). These results indicate that p85α KD increases agonist-stimulated p110α localization along microtubules and MAP4 binding, resulting in its enhanced incorporation in endosomal membranes.

Activated receptor tyrosine kinases undergo rapid internalization, and the endosomal compartments are major platforms for intracellular signaling.[29] As agonist stimulation was required to drive enhanced activation of PI3K/Akt signaling in response to p85α KD, we envisioned that the residual p110α binds activated receptor tyrosine kinases to regulate agonist-activated PI3K/Akt signaling. Although p85α KD reduced p110α levels, much of the residual p110α remained associated with EGFR following EGF stimulation, as demonstrated by coIP, IF, and proximity ligation assays (PLAs) (Figures 4D, 4E, and S3F). Furthermore, the association of residual p110α with IR following insulin stimulation was significantly increased in response to p85α KD (Figure 4F). These results suggest that p85α KD may increase the efficiency of targeting p110α to activated receptors. The increased association of p110α with MAP4 and its distribution along microtubules facilitate the association of residual p110α, presumably coupled to p85β, with activated receptors localized largely on endosomal membranes in response to agonist stimulation and p85α KD. These results are in accord with our recent report regarding the spatial localization of PI3K/Akt signaling predominantly in endosomal compartments downstream of activated receptor tyrosine kinases.[21]

The p110α C2 domain-PI3P interaction promotes agonist-stimulated endosomal PI3K/Akt signaling in response to p85α KD

We next examined the mechanisms by which p110α is recruited to the endosomal compartments following agonist stimulation and p85α KD. The C2 domain of p110α is a presumed membrane-interacting module in PI3Ks[26] that binds the iSH2 domain of p85α by contact at two different sites.[30–32] Moreover, the p85α iSH2 domain partially masks the p110α C2 domain and creates steric hindrances with an anionic phospholipid membrane surface,[14,33] thereby inhibiting p110α interaction with membranes.[30] This suggests that p85α loss may enhance the p110α C2 domain interaction with membranes to regulate PI3K/Akt signaling. Consistent with this idea, ectopically expressed hemagglutinin (HA)-tagged p110α with the C2 domain deleted disrupted its co-localization with the endosomal marker EEA1 compared to wild-type p110α (Figure 5A). Moreover, the C2 domain deletion mutant p110α did not support agonist-stimulated Akt activation following p85α KD (Figure 5B). Furthermore, HA-tagged wild-type p110α, but not the C2 domain deletion mutant p110α (C2 Del HA-p110α), rescued the effects of endogenous p110α KD on agonist-stimulated Akt activation (Figure 5C). Importantly, an *in vitro* lipid kinase assay of the immuno-isolated HA-tagged p110α using a $PI4,5P_2$ substrate showed increased lipid kinase activity of the C2 domain deletion mutant p110α, indicating that C2 domain deletion does not compromise p110α kinase activity *in vitro* (Figure 5D). These results indicate that the C2 domain of p110α is required for its spatial recruitment to endosomal membranes and for enhancing agonist-stimulated Akt activation in response to p85α KD.

To define the critical amino acid residues in the C2 domain of p110α, we mutated the basic residues K410, R412, K413, and K416 in the CBR3 loop of the C2 domain that are the putative membrane-interacting residues[30] and are highly conserved (Figure 5E). The C2 domain assumes a characteristic eight-stranded antiparallel β-sandwich.[30] We performed a lipid overlay assay using the glutathione S-transferase-tagged C2 domain and its 4Q mutant form (K410, R412, K413, and K416 each mutated to Q). The p110α C2 domain, but not its 4Q mutant, bound robustly to PI3P, a critical endosomal phosphoinositide.[16] Pull-down of the C2 domain, but not its corresponding 4Q mutant, by PI3P PolyPIPosome provides compelling evidence of the p110α C2 domain interaction with PI3P (Figure 5F). Additionally, HA-tagged 4Q mutant p110α exhibited impaired endosomal localization (Figure 5G). These mutations severely abrogated the ability of p110α to enhance agonist-stimulated Akt activation following p85α KD (Figures 5G and 5H). Furthermore, these mutations also disrupted the association of p110α with EGFR and the co-localization with endosomal EGFR upon EGF stimulation (Figures 6A–6C). The impaired association of the 4Q mutant p110α with EGFR upon agonist stimulation was further validated by coIP and PLA after transient transfection (Figures 6D–6F). Together, these data indicate that the p110α C2-PI3P interaction is pivotal for bringing p110α to the endomembrane to associate with the activated receptor.

Increased tumorsphere formation induced by stable p85α KD depends on p85β and MAP4

p85α downregulation is associated with oncogenic transformation and increased invasiveness.[9,34,35] We used a lentiviral shRNA system to stably KD p85α in murine mammary epithelial cells (NMuMG) and observed that stable p85α KD resulted in increased

Akt activation, enhanced phosphorylation of downstream mTORC1 target proteins p70S6K1 and 4E-BP-1, and increased cell growth (Figure 6G). These effects were abrogated by PI3Kα inhibitor alpelisib. Furthermore, stable p85α KD in two additional cancer cell lines resulted in increased PI3K/Akt signaling pathway activation (Figures S1D and S1E) and increased tumorsphere formation, and these effects were inhibited by transient KD of p85β or MAP4 (Figures 6H and 6I), consistent with our results demonstrating the critical role of p85β and MAP4 in the augmented agonist-stimulated PI3K/Akt activation in response to p85α loss (Figures 3G and S3D). These results demonstrate that p85α KD promotes tumor cell growth by a MAP4- and p85β-dependent mechanism, thereby providing insights into the tumor-promoting mechanisms of p85α loss.

DISCUSSION

We recently reported that agonist-stimulated $PI3,4,5P_3$ generation and Akt activation occur predominantly at internal membranes.[21] The rapid endocytosis of activated receptor tyrosine kinases and PI3Kα organization along microtubules via MAP4 promotes spatial activation of PI3K/Akt signaling at the endomembrane by facilitating the association of PI3Kα with activated receptor tyrosine kinases.[21] In the current study, we deciphered the comprehensive mechanism by which loss of the p85α adaptor subunit paradoxically elicits enhanced PI3K/Akt signaling downstream of activated receptor tyrosine kinases by emphasizing the inherent capacity of the p110α catalytic subunit for membrane interaction. The organization of p110α along microtubules, p110α recruitment into internal membrane compartments, and p110α association with receptor tyrosine kinase remain completely intact and augmented by p85α KD. Notably, the p110α C2 domain interaction with PI3P guides the spatial recruitment of p110α into endosomes, where the majority of receptor tyrosine kinase remains active after agonist stimulation. As a result, p110α elicits pronounced PI3K/Akt signaling downstream of activated receptor tyrosine kinases in response to p85α loss.

p85α and p85β constituted virtually all the adaptor subunits (~97%) of class IA PI3Ks, with no detectable expression of p55γ in the cell lines used in these experiments. We observed that in response to p85α KD, the majority of p110α associates with p85β. Moreover, p85β KD abrogates the effects of p85α KD in augmenting agonist-stimulated PI3K/Akt signaling, underscoring the key functional role of p85β in the paradoxical PI3K/Akt hyperactivation upon p85α loss. Consistent with these results, p110α coupled with p85β was reported to be more competent at inducing PI3K/Akt signaling.[14] Furthermore, p110β (i.e., PI3Kβ) cannot assume the predominant role in receptor tyrosine kinase-stimulated PI3K/Akt signaling even in the p85α-p110α downregulated condition because of the more stringent constraint imposed on p110β by p85 adaptor subunits.[36] Although p110α devoid of p85α and expressed in mammalian cells, as opposed to in insect or yeast cells, is enzymatically inactive, as demonstrated by *in vitro* kinase assay,[37,38] the residual p110α uncoupled from p85 may also contribute to agonist-stimulated PI3K/Akt signaling upon p85α loss in mammalian cells. It seems plausible that upon p85α loss, residual p110α remains active due to disengaged intermolecular constraints imposed by the p85α nSH2 and iSH2 domains. However, unlike p110α helical domain mutants (e.g., E542K, E545K), which disrupt the p85 nSH2 domain interaction and induce the constitutive activation of PI3K/Akt signaling independent of receptor tyrosine kinase activation,[39] agonist stimulation

is required for the enhanced activation of PI3K/Akt signaling in response to p85α KD. This finding indicates that rapidly internalized active receptor tyrosine kinases in endosomes are indispensable for eliciting the spatial activation of p110α at endomembranes.

By deleting and mutating key basic residues in the C2 domain of p110α, we have demonstrated that the interaction of this domain with the phosphoinositide PI3P is required for its recruitment to endosomal membranes and activating agonist-stimulated PI3K/Akt signaling upon p85α KD. These findings are consistent with the observation that the p85α iSH2 domain partially masks the C2 domain from interacting with membranes.[30] Additionally, the C2 domain mutant p110α (N345K) or deletion of the C-terminal segment of the C2 domain, which disrupts the p85α iSH2 domain interaction, promotes PI3K/Akt signaling.[32] Furthermore, the more negative electrostatic charge distribution in the p85α vs. the p85β iSH2 domain creates a steric hindrance for membrane interaction.[14] Collectively, these studies support a model whereby the p110α C2 domain is not fully exposed for PI3P binding and endosomal recruitment until hindrance from p85α is removed.[21] Upon p85α loss, the resulting enhanced C2-domain-mediated recruitment of p110α to endomembranes promotes its interaction with receptor tyrosine kinases activated by agonist stimulation, resulting in augmented PI3K/Akt signaling. PI3Kα mutants observed in cancer (e.g., activating mutations in the C2 or helical domains) that lose inhibitory contacts and constraints of the p85α adaptor subunit may utilize and exploit enhanced endosomal targeting via the p110α C2-PI3P interaction and/or augmented interaction with scaffolding molecules like MAP4 and IQGAP1 to drive oncogenic PI3K/Akt signaling.[20,21,40] As many components of PI3K/Akt signaling, including activated receptor tyrosine kinases, PI3K, Akt, and mTOR, are localized in endosomes and internal membrane compartments,[41] therapeutic targeting of the molecular interaction of the p110α C2 domain with PI3P could prove to be a promising strategy to disrupt receptor tyrosine kinase-stimulated endosomal PI3K/Akt signaling in cancer, including those with loss or diminished expression of p85α. Indeed, a recent report of an allosteric PI3Kα-activating compound[42] indicates that its binding diminishes p85α interactions with the p110α kinase domain and the inhibitory interface between p85α and the p110α-C2 domain, which would be predicted to enhance p110α interaction with the lipid membrane and PI3P. This mechanism of activation of PI3Kα is fully consistent with our model for p85α/β, MAP4, and PI3P regulation of PI3Kα. Notably, both p85β and MAP4 function as tumor promoters, and MAP4 is overexpressed in different cancer types.[43–45] In summary, the lost or reduced expression of p85α leads to residual p110α coupling with p85β, increased MAP4 interaction, enhanced integration to endosomal membranes, and increased interaction with activated receptors, all resulting in increased agonist-stimulated PI3K/Akt signaling. Finally, the observation that the tumor-promoting effects of p85α KD, which mimics the reduced expression of p85α in some human tumors, are dependent on p85β and MAP4 implicates these molecules as potential therapeutic targets in these tumors.

Limitations of the study

This study presents data utilizing multiple approaches to uncover the mechanisms underlying the paradoxical augmented PI3K/Akt activation in response to p85α loss, yet there are limitations. First, the analysis of mass spectrometry data indicated the existence

of p85 adaptor-free p110α. However, more rigorous and detailed analyses will be required to either prove or disprove the existence of p85 adaptor-free p110α in physiologically relevant cellular contexts. Second, the overexpression of different mutant forms of p85α eliciting PI3K/Akt signaling has been observed in human tumors (e.g., endometrial cancer). The mechanisms by which the p85α mutant results in augmented PI3K/Akt signaling need to be carefully examined in further studies. Third, the detailed intermolecular interactions between residual p110α in complex with p85β, MAP4, and IQGAP1 and their integration into endosomal membranes via PI3P interaction will require biochemical and structural approaches to map the precise amino acid residues required to regulate these critical interactions and illuminate their functional roles in regulating agonist-stimulated PI3K/Akt signaling in the setting of p85α loss.

STAR★METHODS

RESOURCE AVAILABILITY

Lead contact—Further information and requests for resources and reagents should be directed to and will be fulfilled by the lead contact, Dr. Richard A Anderson (raanders@wisc.edu).

Materials availability

- Plasmids generated in this study will be deposited to Addgene and can also be obtained by contacting the lead contact.
- Cell lines with stable expression of the HA-tagged p110α constructs or stable knockdown of p85α can be obtained by contacting the lead contact.
- This study did not generate other new and unique reagents.

Data and code availability

- Availability of Data: All the raw data used to generate the graphs in this study are stored and will be made made available upon reasonable requests. Mass spectrometry data of the HA-p110α immunoprecipitates from control vs. p85α KD MDA-MB-231 cells are available via ProteomeXchange with identifier ProteomeXchange: PXD050817. All the confocal microscopy data reported in this paper are stored in Optical Imaging Core Facility at UW-Madison and will be shared by the lead contact upon a reasonable request.
- This paper does not report the original code.
- Any additional information required to reanalyze the data reported in this paper is available from the lead contact upon request.

EXPERIMENTAL MODEL AND STUDY PARTICIPANT DETAILS

Cell culture—MDA-MB-231, A431, H4, HCT116, HEK293T and COS-7 were purchased from American Type Culture Collection (ATCC). All cell lines were cultured in DMEM-containing 10% FBS (Hyclone) and antibiotics (penicillin/streptomycin) at 37°C in a 5% CO_2 incubator. NMuMG, murine mammary epithelial cells were cultured in DMEM-

containing 10% FBS (Hyclone) and antibiotics (penicillin/streptomycin) supplemented by 10 μg/mL insulin as previously.[46] All cell lines were routinely tested for the mycoplasma contamination and sub-cultured before reaching 80–90% of confluency. Cells were cultured and passaged continuously for not more that 2 months. After that, fresh stock of cells from liquid nitrogen were revived and cultured.

siRNA-mediated knockdown—For siRNA-mediated knockdown of protein expression, cells were seeded 12–18 h before the cell transfection. LipofectamineRNAiMAX (#13778150, Invitrogen) was used following the protocol provided by the manufacturer, and cells were assayed 48–72 h post-transfection.

Plasmids transfection—For plasmid transfections, cells were seeded 12–18 h before the cell transfection. Lipofectamine-3000 (#L3000015, Invitrogen) was used following the protocol provided by the manufacturer, and cells were harvested 24–48 h post-transfection.

Lentiviral-mediated ectopic gene expression—The expression of the HA-tagged p110α (wild type), C2 deletion mutant (p110α C2 Del.) and p110α 4Q mutant in MDA-MB-231 cells were carried out by lentiviral-mediated ectopic gene expression as described previously.[47] Briefly, for the generation of the infectious viral particles, cDNAs for the indicated contructs cloned into pWPT-GFP lentiviral vector were transfected along with the accessory plasmids, psPAX2 and pMD2.G (Addgene) into HEK 293T cells using calcium phosphate. Conditioned medium was collected 48 h post-transfection, cleared of debris by centrifugation at low speed, filtered through 0.45 μM filter and viral particles were concentrated by centrifugation at 24,000 rpm in Beckman SW28 centrifuge for 2 h at 4°C. The concentrated viral particles either used to infect the target cells, MDA-MB-231 or stored at −80°C for later use. Alternatively, the conditioned medium containing the infectious viral paricles were used directly without concentrating the virus partcilces. For the transduction of the target cells, the cells were sub-cultured 12–18 h before the infection in the presence of 0.5 μg/mL polybrene (Sigma). The indicated gene expression were anylazed 48–72 h post-infection. The target cells stably expressing the indicated genes were identified by individual clone selections and the pool of more than 10 clones used for the experiments.

shRNA-mediated knockdown—The stable knockdown of p85α in MDA-MB-231, A431 and NMuMG cells were carried out using lentiviral shRNA system. For this, control shRNA lentiviral particles (sc-108080), human p85αshRNA lentiviral particles (sc-36217-v) and murine p85αshRNA lentiviral particles (sc-36218-v), all transduction-ready viral particles were purchased from Santa Crutz Biotechnologies and used following the shRNA lentiviral particles transduction protocol. For this, target cells seeded 12–18 h before viral transduction were infected with lentiviral particles in fresh and complete growth medium containing 5 μg/mL of Polybrene. After 2–3 days, cells were replated and allowed to grow in complete growth medium containing the puromycin dihydrochloride (0.5 μg/mL). The transduced and puromycin-resistant cells growing in the culture plates were refed with fresh growth medium containing the puromycin selection marker. After 7 days, puromycine-resistant cells remaining in the culture plate were harvested and replated in new culture plates for further propagation as well as to analyze p85α knockdown by western blotting.

After confirming the p85α KD in the pool of puromycin-resistant cells, the cells were used for the experiments.

Tumorsphere formation—The single cells were suspended in complete growth medium containing 0.25% Matrigel (Cat#356231, Corning) and seeded into ultralow attachment culture plates (Costar Cat#3473) at the concentration of $1x10^3$ cells/well. The 3–4 days later, cells were suppletemented with 250 μL of fresh growth medium on the top layer and allowed to grow for additional 3–4 days before examining and counting the spheres or tumorsphere formed.

Cell proliferation by manual cell counting—The equal number of conshRNA or p85α shRNA cells ($1x10^5$ cells/well) were seeded into 6-well culture plate in the complete growth medium. After 72-h, the cells growing in the culture plates were collected by trypsinization and counted manually using Neubauer counting chamber.

METHOD DETAILS

Agonist stimulation of cells—For examination of the phosphorylation levels of Akt and other components of pathway (e.g., PDK1 and mTOR) or PI3,4,5P_3 generation, cells were serum starved overnight before agonist stimulation. Different agonist used were EGF (50 ηg/ml) or insulin (10 μg/mL) or PDGF (10 ηg/ml) or FBS (10%). The cells were harvested at different time points following agonist stimulation as described previously.[21,48]

Immunoprecipitation and immunoblotting—For immunoprecipitation, the cells were often grown and harvested from 10 cm culture dishes. Before cell lysis, cells were washed with cold 1x PBS 2 times. Cells were lysed using lysis buffer (50 mM Tris-HCl pH 7.4, 150 mM, 1% Triton X-100, 1 mM EDTA, 1 mM EGTA and protease/phosphatase inhibitors). The clear supernatants were obtained by centrifuging at 14,000 rpm at 4°C. Clear supernatants were incubated with antibody-coated agarose beads or control beads overnight at 4°C. If nascent antibodies were used, protein-antibody complexes were isolated using protein G or A Sepharose 4B beads (Amersham). Beads were washed three times with lysis buffer before eluting the immunocomplexes with 2x sample buffer, run through SDS-PAGE gel and subjected to immunoblotting using specific antibodies. For immunoblotting/western blotting, primary antibodies were diluted 1:2000 in 3% BSA in TBS-T (0.1% Tween 20). This was followed by incubation with HRP-labelled secondary antibodies. The images were acquired using LI-COR Odyssey FC.

Small interfering RNA (siRNA)—Control siRNA (siCon):5′-UUUCCGCACUGUGAUUCGG-3’.

sip85α I: 5′-GGAUCAAGUUGUCAAAGAA-3’.

sip85α II: 5′-GCAGCUGAGUAUCGAGAAA-3’.

sip85α III: 5′-GGGTGACATATTGACTGTGAATAAA-3’.

siPTEN: 5′-GCUUGAAGACUAAAGCAUA-3’.

sip110α: 5′-UCAAGAAGAAAGCUGACCAUGCUGC-3’.

sip110β: 5′-GCUUCAGAUUUGGCCUAAA-3’.

siMAP4: 5′-CCGGGAACUCAGAGUCAAA-3’.

sip85β was purchased from Dharmacon (Cat#L-003021-00-0005).

These siRNA oligonucleotides were designed using Invitrogen Block-iT RNAi Designer and purchased from Thermo Fisher or Dharmacon. For all the experiments with p85α KD, sip85α I siRNA were used.

Immunofluorescence (IF) staining and confocal microscopy—For immunofluorescence study, cells were grown on glass coverslips. Cells were fixed with 4% PFA followed by permeabilization with 0.1% Triton X-100 and blocking with 3% BSA in TBS. Cells were incubated with a primary antibody overnight at 4°C followed by incubation with fluorescent-conjugated secondary antibodies (Molecular Probes) for 1 h at room temperature. Cells were mounted in Prolong Glass Antifade Mounting media (#P36984, Thermo Fisher Scientific). The images were taken by Leica SP8 3X STED Super-Resolution Microscope, which is both a point scanning confocal and 3X STED super-resolution microscope. The Leica SP8 3X STED microscope was controlled by LAS-X software (Leica Microsystems). Images were acquired using 60x or 100x objective lens. Only the image in Figure 4A were taken by Nikon TE2000-U and image processed using Metamorph. For quantification of fluorescence intensity, the mean fluorescent intensity of interested channels in each cell (at least 20 cells used) was measured by LAS-X. The images were processed using ImageJ.

For the investigation of activated Akt or PI3,4,5P_3 lipid messenger generated by immunofluorescence study, the cells growing in the coverslips were stimulated with EGF stimulation followed by rapid fixation with 4% PFA prepared in TBS, and phosphatase inhibitors (2.5 mM NaF and 2.5 mM Na3VO4) were included in the TBS used for incubation of antibodies and washing. For the immunofluorescence staining of MAP4, cells were fixed in ice-cold methanol and anti-MAP4 antibody (#sc-390286, Santa Cruz) was used. Following 3-times washing with TBS, cells were permeabilized with 0.1% Triton X-100 in TBS-containing phosphatase inhibitors. Then, cells were incubated in the blocking buffer containing 3% BSA in TBS for 1 h at room temperature followed by overnight incubation with primary antibody (prepared in TBS-T containing 3% BSA) at 4°C in humidified chamber. Cells were washed 3 times with TBS-T (TBS-containing 0.1% Tween 20) followed by incubation with secondary antibody for 1 h. Cells were washed 3 times before mounting.

Examination of activated Akt in endosomes—For endosome isolation, cells grown in 10 cm culture plates were used. Cells after EGF stimulation, cells were fractionated using an endosome isolation kit (ED-028, Invent Biotechnologies). Briefly, cells were washed with cold TBS on ice before detaching the cells with Trypsin-EDTA. Then, collected cells were suspended in buffer A. The cell suspension were passed through the column. Then, the cell supernatant was centrifuged at 14,000 rpm for 1 h and at first to remove the

plasma membrane/larger organelles before using supernatant for endosome isolation. The equal amount of isolated plasma membrane/larger organelles vs. endosomal fractions were run through SDS-PAGE and immunoblotted with activated Akt and markers for plasma membrane and endosomes.

For examining the activation level of the Akt in different subcellular fractions, A431 cells (conshRNA vs. p85αshRNA) growing in 10 cm culture plates were stimulated with EGF (50 ηg/ml) for 5 min before harvesting the cells. The same endosome isolation kit (ED-028, Invent Biotechnologies) were used to examine the activation level of the Akt in different subcellular fractions. For this, the initial cell fractions enriched with cell nuclei were collected and stored after washing with TBS. Then, cell supernatant was centrifuged at 14,000 rpm for 1 h at 4°C to obtain the cell fraction enriched with plasma membrane and larger organelles. Then, remaining fraction were mixed with buffer B and incubated for 2 h at 4°C before centrifuging at 14,000 rpm for 1 h at 4°C. The endosomal fraction were recovered as pellete and remaining fraction were used as cytosolic fraction.

Semiquantitative mass spectrometry analysis of p110α immunocomplex from p85α KD cells—MDA-MB-231 cells stably expressing the HA-p110α and grown in 15 cm culture plates were used. Cells were transfected with p85α siRNA and used 48–72 h-post transfection. Cells were lysed using lysis buffer (50 mM Tris-HCl [pH 7.4], 150 mM NaCl, 0.5% Triton X-100, 1 mM EDTA, 10 mM NaF and 5 mM Na3VO4) containing protease/phosphatase inhibitors (Roche). Cells were incubated in lysis buffer for 2–3 h in rotator at 4°C. After centrifuging at 14,000 rpm for 15 min, the clear cell lysates were used to immune-precipitate HA-p110α using HA agarose beads. Isolated immunocomplex were eluted using 2x sample buffer without dye. The immunocomplexes obtained from mock or control siRNA or p85α KD cells were analyzed at the mass spectrometry facility of UW-Madison Biotech Center. The spectral count of the p110α, p85α, and p85β peptides obtained were used for the analysis. However, p55γ was not detected in MDA-MB-231 cells by mass spectrometry analysis.

Lipid overlay assay—PIP Strips membranes (#P-6001, Echelon Biosciences) were blocked with 3% fatty acid free BSA (#A7030, Sigma) in TBS for 1–2 h at room temperature. After blocking, the membrane was incubated with purified GST-fusion proteins (GST alone, GST-C2 and GST-C2 4Q) diluted in 3 mL TBS-T 3% BSA at the concentration of 0.2 μg/mL. The membrane was washed with 5 mL TBS-T three times with gentle agitation for 10 min each. This was followed by incubation with anti-GST-HRP antibody diluted in TBS-T 3% BSA for 1 h in room temperature. The membrane was washed 3–5 times with TBS-T before examining the bound GST-fusion protein using ECL detection system.

PI3P PolyPIPosome binding assay—Purified GST-fusion proteins of the p110 α C2 domain (WT GST-C2 or 4Q mutant GST-C2) were incubated with 12 μL PI3P PolyPIPosome (Echelon Biosciences) for 60 min at 4°C in binding buffer (50 mM HEPES, pH 7.4, 150 mM NaCl, 2 mM EGTA, 2 mM $MgCl_2$ and 1% glycerol). PolyPIPosomes were isolated by centrifuging at 14,000 rpm at 4°C and washed three times with binding buffer. The protein bound to PolyPIPosome was analyzed by WB using anti-GST-HRP antibody.

***In vitro* lipid kinase assay using PI4,5P_2 micelles—**HA-tagged p110α was immune-isolated from MDA-MB-231 cells stably expressing the wild type HA-p110α or C2 deletion p110α using HA antibody agarose beads (ThermoFisher). Beads were washed three times with cell lysis buffer and two times with kinase reaction buffer (20 mM HEPES pH 7.4, 100 mM Nacl, 1% BSA, 2 mM $Mgcl_2$, 2 mM DTT and 100 μM ATP). For preparation of PI4,5P_2 micelles, bovine brain PI4,5P_2 power was dissolved in ultra-pure water (2 mg/mL) and allowed to hydrate for 1 h at room temperature. Then, the PI4,5P_2 mixture was sonicated gently until it appear clear. For lipid kinase reaction, prepared PI4,5P_2 micelles were diluted with 2x kinase reaction buffer and 30 μL of lipid mixture added to immuno-isolated HA-p110α coupled in beads. The lipid kinase reaction mix was incubated for 1 h at room temperature. The same lipid mixture with or without commercially available PI3Kα holoenzyme was also used as positive and negative controls, respectively. After 1 h, the lipid mixture was separated from immuno-isolated HA-p110α coupled in beads and mixed with 60 μL of methanol:chloroform:HCl (60:40:1). The lipid dissolved in chloroform was separated by centrifuging the mixture at 12,000 rpm for 10 min. The dissolved lipid in chloroform appearing at the bottom was carefuly pipetted and immediately spotted on a nitrocellulose membrane. The membrane was allowed to dry for 1 h at room temperature before soaking in methanol and the membrane was then washed with TBS buffer 3-times. For the detection of the PI3,4,5P_3 generated, the membrane was incubated overnight at 4°C with PI3,4,5P_3 Grip, GST-Grp1-PH (Echelone) at a concentration of 0.5 μg/mL in TBS buffer with 3% BSA. The GST-Grp1-PH bound to the PI3,4,5P_3 generated and spotted on the membrane was detected using HRP-labelled anti-GST antibody.

Proximity ligation assay (PLA)—PLA was applied to detect *in situ* protein-protein interaction as described previously.[21,48] Cells after fixation and permeabilization were blocked before incubation with primary antibodies as in the routine IF staining procedure. After that, the cells were processed for PLA (#DUO92101, Millipore Sigma) according to the manufacturer's instruction and previously. PLA signals are detected by Leica SP8 confocal microscope as discrete punctate foci and provide the intracellular localization of the protein-protein complex and were later quantified by ImageJ.

Subcloning of human p110α and its constructs into PWPT-GFP lentiviral vector—The cDNA for human p110α was a kind gift of Dr. Peter K. Vogt (Scripps Research Institute). The detailed procedure for subcloning of p110α in frame with HA-tag at N terminus of pWPT-GFP lentiviral vector has been described previously.[21] Similarly, the generation of C2 domain deletion mutant of p110α has also been described previously.[21] For the generation of p110α 4Q mutant, p110α cDNA was cloned, at first into SalI and XhoI sites of pCMV-HA vector using primers: 5′-AAAGTCGACCATGCCTCCACGACCATCATC-3′ and 5′-AAACTCGAGTCAGTTCAATGCATGCTGT-3'. Then, C2 domain residues Lys^{410}, Arg^{412}, Lys^{413} and Lys^{416} were mutated to Glutamine (Q) in two steps. At first, the mutation on Lys^{410} and Lys^{416} were created using primers: 5′-TGCTCTGTTCAAGGCCGAAAGGGTGCTCAAGAGGAAC-3′ and 5′-GTTCCTCTTGAGCACCCTTTCGGCCTTGAACAGAGCA-3'. This mutant was used as a template to generate remaining mutation in Arg^{412} and Lys^{413} using a second

set of primers: 5′-TGCTCTGTTCAAGGCCAACAGGGTGCTCAAGAGGAAC-3′ and 5′-TGCTCTGTTCAAGGCCAACAGGGTGCTCAAGAGGAAC-3’. The generated 4Q mutant p110α in pCMV-HA vector was further subcloned into pWPT-GFP lentiviral vector as described previously.[21,47] The mutations created and integrity of DNA were confirmed by DNA sequencing.

Cloning of C2 domain and its mutant form into pGEX-6p-1 vector and protein purification—The PCR products for p110α C2 domain and its 4Q mutant form were generated by using the primers: 5′-AAAGGATCCAGTGCACTCAGAATAAA-3′ and 5′-AAACTCGAGTCATTATAGTCTGTTACTCAGTC-3’. The amplified PCR products were subcloned into BamH1 and XhoI sites of pGEX-6p-1 vector (Amersham). The integrity of DNA sequences was validated by DNA sequencing.

The *E. coli* BL21 (DE3) (Thermo Fisher Scientific) were used for the expression of the GST-fusion proteins. Almost all expressed proteins were recovered in the insoluble fractions (inclusion bodies). To recover proteins in soluble fraction, we induced the expression of each protein at 25°C by culturing the bacteria (2 L of LB medium for each protein) for 48 h in the presence of 0.1 mM of isopropyl-β-D-thiogalactoside (IPTG) and osmotic stress (330 mM sorbitol and 2.5 mM betaine) as described previously.[21] Proteins were purified from soluble fractions of the bacterial cell lysates using Glutathione Sepharose beads (GE Healthcare). Proteins were dialyzed in 1x TBS overnight at 4°C overnight and protein quantified. The integrity and purity of purified GST-fusion proteins were examined by running 1 μg of proteins through 12% SDS-PAGE gel followed by Coomassie staining.

QUANTIFICATION AND STATISTICAL ANALYSIS

Data are presented as mean ± SD from at least three independent experiments with similar results. At least three western blot images from three independent experiments were used to generate the graphs and unpaired t test was conducted to determine the *p*-value between the two groups. All the micrographs (IF images) are the representative images of three representative experiments as indicated in each figure legend. For the quantification of immunofluorescence images, the number of cells used for each representative experiment is indicated and unpaired t test was conducted to determine the *p*-value between the two groups. The *p*-value less than 0.05 were considered significant between two groups.

Supplementary Material

Refer to Web version on PubMed Central for supplementary material.

ACKNOWLEDGMENTS

We thank members of the Anderson and Cryns lab for comments, Dr. Adrea Galmozzi for discussions and comments, and Lance Rodenkirch for technical support. This work was supported by a National Institutes of Health grant R35GM134955 (R.A.); a National Institutes of Health grant 5R21AG074605-02 (N.T. and R.A.); Department of Defense Breast Cancer Research Program grants W81XWH-17-1-0258, HT9425-23-1-0554, and AAM4185 (R.A.) and HT9425-23-1-0553 and W81XWH-21-1-0129 (V.L.C.); and a grant from the Breast Cancer Research Foundation (V.L.C.).

REFERENCES

1. Tsolakos N, Durrant TN, Chessa T, Suire SM, Oxley D, Kulkarni S, Downward J, Perisic O, Williams RL, Stephens L, and Hawkins PT (2018). Quantitation of class IA PI3Ks in mice reveals p110-free-p85s and isoform-selective subunit associations and recruitment to receptors. Proc. Natl. Acad. Sci. USA 115, 12176–12181. [PubMed: 30442661]
2. Rathinaswamy MK, and Burke JE (2020). Class I phosphoinositide 3-kinase (PI3K) regulatory subunits and their roles in signaling and disease. Adv. Biol. Regul. 75, 100657.
3. Burke JE (2018). Structural Basis for Regulation of Phosphoinositide Kinases and Their Involvement in Human Disease. Mol. Cell 71, 653–673. [PubMed: 30193094]
4. Manning BD, and Toker A. (2017). AKT/PKB Signaling: Navigating the Network. Cell 169, 381–405. [PubMed: 28431241]
5. Mauvais-Jarvis F, Ueki K, Fruman DA, Hirshman MF, Sakamoto K, Goodyear LJ, Iannacone M, Accili D, Cantley LC, and Kahn CR (2002). Reduced expression of the murine p85alpha subunit of phosphoinositide 3-kinase improves insulin signaling and ameliorates diabetes. J. Clin. Invest. 109, 141–149. [PubMed: 11781359]
6. Terauchi Y, Tsuji Y, Satoh S, Minoura H, Murakami K, Okuno A, Inukai K, Asano T, Kaburagi Y, Ueki K, et al. (1999). Increased insulin sensitivity and hypoglycaemia in mice lacking the p85 alpha subunit of phosphoinositide 3-kinase. Nat. Genet. 21, 230–235. [PubMed: 9988280]
7. Ueki K, Yballe CM, Brachmann SM, Vicent D, Watt JM, Kahn CR, and Cantley LC (2002). Increased insulin sensitivity in mice lacking p85beta subunit of phosphoinositide 3-kinase. Proc. Natl. Acad. Sci. USA 99, 419–424. [PubMed: 11752399]
8. Taniguchi CM, Winnay J, Kondo T, Bronson RT, Guimaraes AR, Alemán JO, Luo J, Stephanopoulos G, Weissleder R, Cantley LC, and Kahn CR (2010). The phosphoinositide 3-kinase regulatory subunit p85alpha can exert tumor suppressor properties through negative regulation of growth factor signaling. Cancer Res. 70, 5305–5315. [PubMed: 20530665]
9. Thorpe LM, Spangle JM, Ohlson CE, Cheng H, Roberts TM, Cantley LC, and Zhao JJ (2017). PI3K-p110alpha mediates the oncogenic activity induced by loss of the novel tumor suppressor PI3K-p85alpha. Proc. Natl. Acad. Sci. USA 114, 7095–7100. [PubMed: 28630349]
10. Wang J, Zhang N, Peng M, Hua X, Huang C, Tian Z, Xie Q, Zhu J, Li J, Huang H, and Huang C. (2019). p85alpha Inactivates MMP-2 and Suppresses Bladder Cancer Invasion by Inhibiting MMP-14 Transcription and TIMP-2 Degradation. Neoplasia 21, 908–920. [PubMed: 31401412]
11. Chen Y, Zeng C, Zhan Y, Wang H, Jiang X, and Li W. (2017). Aberrant low expression of p85alpha in stromal fibroblasts promotes breast cancer cell metastasis through exosome-mediated paracrine Wnt10b. Oncogene 36, 4692–4705. [PubMed: 28394344]
12. Ito Y, Hart JR, Ueno L, and Vogt PK (2014). Oncogenic activity of the regulatory subunit p85beta of phosphatidylinositol 3-kinase (PI3K). Proc. Natl. Acad. Sci. USA 111, 16826–16829. [PubMed: 25385636]
13. Ito Y, Vogt PK, and Hart JR (2017). Domain analysis reveals striking functional differences between the regulatory subunits of phosphatidylinositol 3-kinase (PI3K), p85alpha and p85beta. Oncotarget 8, 55863–55876. [PubMed: 28915558]
14. Vallejo-Díaz J, Chagoyen M, Olazabal-Morán M, González-García A, and Carrera AC (2019). The Opposing Roles of PIK3R1/p85alpha and PIK3R2/p85beta in Cancer. Trends Cancer 5, 233–244. [PubMed: 30961830]
15. Liu Z, and Roberts TM (2006). Human tumor mutants in the p110alpha subunit of PI3K. Cell Cycle 5, 675–677. [PubMed: 16627990]
16. Dickson EJ, and Hille B. (2019). Understanding phosphoinositides: rare, dynamic, and essential membrane phospholipids. Biochem. J. 476, 1–23. [PubMed: 30617162]
17. Vadas O, Burke JE, Zhang X, Berndt A, and Williams RL (2011). Structural basis for activation and inhibition of class I phosphoinositide 3-kinases. Sci. Signal. 4, re2.
18. Lemmon MA (2008). Membrane recognition by phospholipid-binding domains. Nat. Rev. Mol. Cell Biol. 9, 99–111. [PubMed: 18216767]
19. Corbalan-Garcia S, and Gómez-Fernández JC (2014). Signaling through C2 domains: more than one lipid target. Biochim. Biophys. Acta 1838, 1536–1547. [PubMed: 24440424]

20. Choi S, Hedman AC, Sayedyahossein S, Thapa N, Sacks DB, and Anderson RA (2016). Agonist-stimulated phosphatidylinositol-3,4,5-trisphosphate generation by scaffolded phosphoinositide kinases. Nat. Cell Biol. 18, 1324–1335. [PubMed: 27870828]
21. Thapa N, Chen M, Horn HT, Choi S, Wen T, and Anderson RA (2020). Phosphatidylinositol-3-OH kinase signalling is spatially organized at endosomal compartments by microtubule-associated protein 4. Nat. Cell Biol. 22, 1357–1370. [PubMed: 33139939]
22. Chen M, Choi S, Jung O, Wen T, Baum C, Thapa N, Lambert PF, Rapraeger AC, and Anderson RA (2019). The Specificity of EGF-Stimulated IQGAP1 Scaffold Towards the PI3K-Akt Pathway is Defined by the IQ3 motif. Sci. Rep. 9, 9126. [PubMed: 31235839]
23. Geering B, Cutillas PR, Nock G, Gharbi SI, and Vanhaesebroeck B. (2007). Class IA phosphoinositide 3-kinases are obligate p85-p110 heterodimers. Proc. Natl. Acad. Sci. USA 104, 7809–7814. [PubMed: 17470792]
24. Geering B, Cutillas PR, and Vanhaesebroeck B. (2007). Regulation of class IA PI3Ks: is there a role for monomeric PI3K subunits? Biochem. Soc. Trans. 35, 199–203. [PubMed: 17371237]
25. Rabinovsky R, Pochanard P, McNear C, Brachmann SM, Duke-Cohan JS, Garraway LA, and Sellers WR (2009). p85 Associates with unphosphorylated PTEN and the PTEN-associated complex. Mol. Cell Biol. 29, 5377–5388. [PubMed: 19635806]
26. Bilanges B, Posor Y, and Vanhaesebroeck B. (2019). PI3K isoforms in cell signalling and vesicle trafficking. Nat. Rev. Mol. Cell Biol. 20, 515–534. [PubMed: 31110302]
27. Jethwa N, Chung GHC, Lete MG, Alonso A, Byrne RD, Calleja V, and Larijani B. (2015). Endomembrane PtdIns(3,4,5)P3 activates the PI3K-Akt pathway. J. Cell Sci. 128, 3456–3465. [PubMed: 26240177]
28. Sato M, Ueda Y, Takagi T, and Umezawa Y. (2003). Production of PtdInsP3 at endomembranes is triggered by receptor endocytosis. Nat. Cell Biol. 5, 1016–1022. [PubMed: 14528311]
29. Murphy JE, Padilla BE, Hasdemir B, Cottrell GS, and Bunnett NW (2009). Endosomes: a legitimate platform for the signaling train. Proc. Natl. Acad. Sci. USA 106, 17615–17622. [PubMed: 19822761]
30. Huang CH, Mandelker D, Schmidt-Kittler O, Samuels Y, Velculescu VE, Kinzler KW, Vogelstein B, Gabelli SB, and Amzel LM (2007). The structure of a human p110alpha/p85alpha complex elucidates the effects of oncogenic PI3Kalpha mutations. Science 318, 1744–1748. [PubMed: 18079394]
31. Liu S, Knapp S, and Ahmed AA (2014). The structural basis of PI3K cancer mutations: from mechanism to therapy. Cancer Res. 74, 641–646. [PubMed: 24459181]
32. Wu H, Shekar SC, Flinn RJ, El-Sibai M, Jaiswal BS, Sen KI, Janakiraman V, Seshagiri S, Gerfen GJ, Girvin ME, and Backer JM (2009). Regulation of Class IA PI 3-kinases: C2 domain-iSH2 domain contacts inhibit p85/p110alpha and are disrupted in oncogenic p85 mutants. Proc. Natl. Acad. Sci. USA 106, 20258–20263. [PubMed: 19915146]
33. Zhang M, Jang H, and Nussinov R. (2019). The mechanism of PI3Kalpha activation at the atomic level. Chem. Sci. 10, 3671–3680. [PubMed: 30996962]
34. Liu B, Fang X, Kwong DLW, Zhang Y, Verhoeft K, Gong L, Zhang B, Chen J, Yu Q, Luo J, et al. (2022). Targeting TROY-mediated P85a/AKT/TBX3 signaling attenuates tumor stemness and elevates treatment response in hepatocellular carcinoma. J. Exp. Clin. Cancer Res. 41, 182. [PubMed: 35610614]
35. Wu T, Song H, Xie D, Zhao B, Xu H, Wu C, Hua K, Deng Y, Ji C, Hu J, and Fang L. (2018). Silencing of ASPP2 promotes the proliferation, migration and invasion of triple-negative breast cancer cells via the PI3K/AKT pathway. Int. J. Oncol. 52, 2001–2010. [PubMed: 29568874]
36. Zhang X, Vadas O, Perisic O, Anderson KE, Clark J, Hawkins PT, Stephens LR, and Williams RL (2011). Structure of lipid kinase p110beta/p85beta elucidates an unusual SH2-domain-mediated inhibitory mechanism. Mol. Cell 41, 567–578. [PubMed: 21362552]
37. Klippel A, Escobedo JA, Hirano M, and Williams LT (1994). The interaction of small domains between the subunits of phosphatidylinositol 3-kinase determines enzyme activity. Mol. Cell Biol. 14, 2675–2685. [PubMed: 8139567]

38. Hiles ID, Otsu M, Volinia S, Fry MJ, Gout I, Dhand R, Panayotou G, Ruiz-Larrea F, Thompson A, and Totty NF (1992). Phosphatidylinositol 3-kinase: structure and expression of the 110 kd catalytic subunit. Cell 70, 419–429. [PubMed: 1322797]

39. Burke JE, Perisic O, Masson GR, Vadas O, and Williams RL (2012). Oncogenic mutations mimic and enhance dynamic events in the natural activation of phosphoinositide 3-kinase p110alpha (PIK3CA). Proc. Natl. Acad. Sci. USA 109, 15259–15264. [PubMed: 22949682]

40. Jenkins ML, Ranga-Prasad H, Parson MAH, Harris NJ, Rathinaswamy MK, and Burke JE (2023). Oncogenic mutations of PIK3CA lead to increased membrane recruitment driven by reorientation of the ABD, p85 and C-terminus. Nat. Commun. 14, 181. [PubMed: 36635288]

41. Thapa N, Horn HT, and Anderson RA (2019). Phosphoinositide spatially free AKT/PKB activation to all membrane compartments. Adv. Biol. Regul. 72, 1–6. [PubMed: 30987931]

42. Gong GQ, Bilanges B, Allsop B, Masson GR, Roberton V, Askwith T, Oxenford S, Madsen RR, Conduit SE, Bellini D, et al. (2023). A small-molecule PI3Kalpha activator for cardioprotection and neuroregeneration. Nature 618, 159–168. [PubMed: 37225977]

43. Zeng W, Xu H, Wei T, Liang H, Ma X, and Wang F. (2022). Overexpression of BRINP3 Predicts Poor Prognosis and Promotes Cancer Cell Proliferation and Migration via MAP4 in Osteosarcoma. Dis. Markers 2022, 2698869.

44. Zhang S, Deen S, Storr SJ, Yao A, and Martin SG (2019). Expression of Syk and MAP4 proteins in ovarian cancer. J. Cancer Res. Clin. Oncol. 145, 909–919. [PubMed: 30737623]

45. Jiang YY, Shang L, Shi ZZ, Zhang TT, Ma S, Lu CC, Zhang Y, Hao JJ, Shi C, Shi F, et al. (2016). Microtubule-associated protein 4 is an important regulator of cell invasion/migration and a potential therapeutic target in esophageal squamous cell carcinoma. Oncogene 35, 4846–4856. [PubMed: 26876215]

46. Thapa N, Tan X, Choi S, Wise T, and Anderson RA (2017). PIPKI-gamma and talin couple phosphoinositide and adhesion signaling to control the epithelial to mesenchymal transition. Oncogene 36, 899–911. [PubMed: 27452517]

47. Thapa N, Sun Y, Schramp M, Choi S, Ling K, and Anderson RA (2012). Phosphoinositide signaling regulates the exocyst complex and polarized integrin trafficking in directionally migrating cells. Dev. Cell 22, 116–130. [PubMed: 22264730]

48. Chen M, Choi S, Wen T, Chen C, Thapa N, Lee JH, Cryns VL, and Anderson RA (2022). A p53-phosphoinositide signalosome regulates nuclear AKT activation. Nat. Cell Biol. 24, 1099–1113. [PubMed: 35798843]

Highlights

- Loss of p85α promotes the coupling of residual p110α with p85β
- The p110α-p85β complex has increased endosomal and receptor association
- The p110α C2 domain interacts with PI3P for endosomal targeting
- p110α C2 domain/PI3P interaction is required for agonist-stimulated PI3K activation

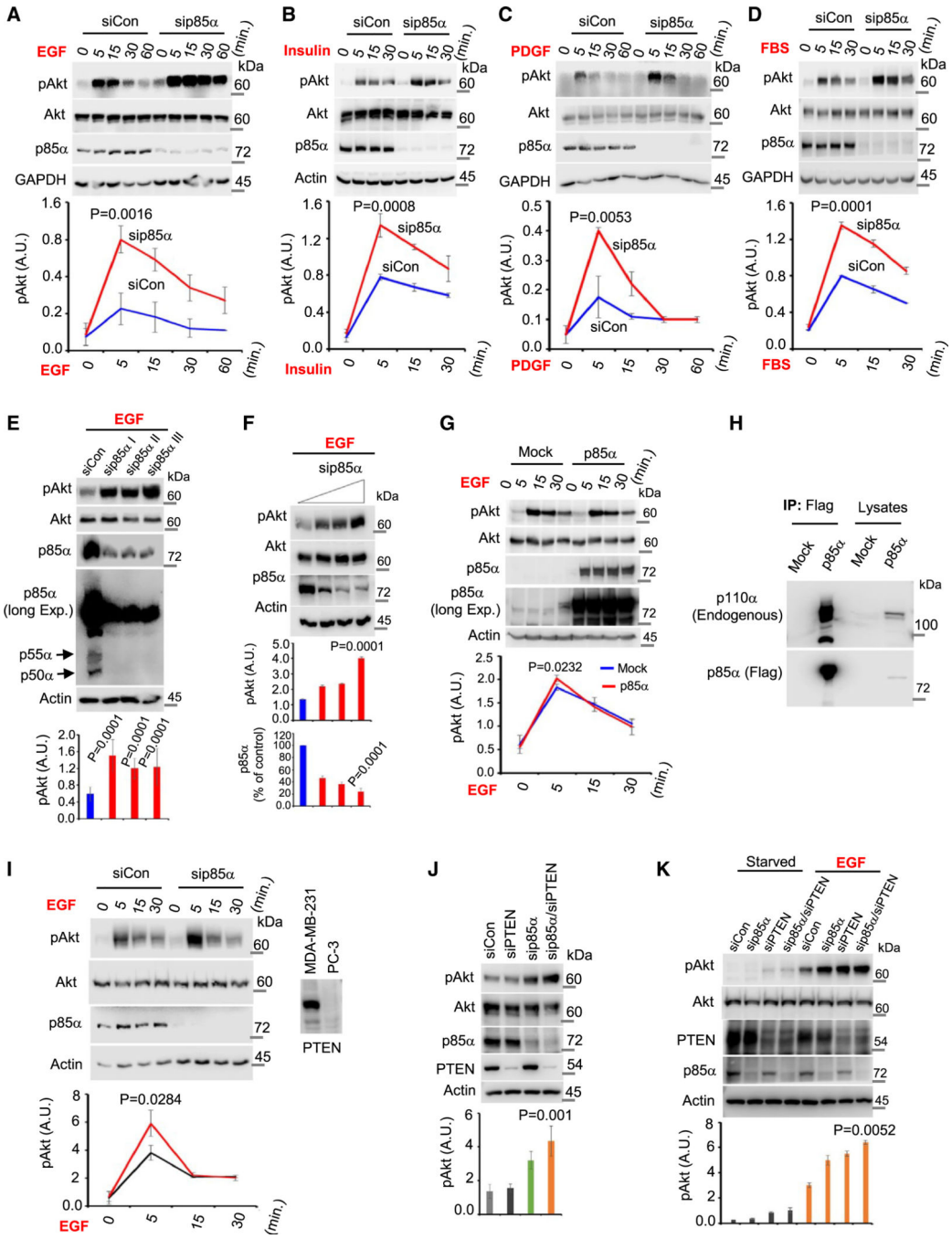

Figure 1. p85α KD promotes Akt activation downstream of activated receptor tyrosine kinases

(A–D) p85α KD promotes agonist-stimulated Akt activation. MDA-MB-231 cells were transfected with either control siRNAs or siRNAs targeting all the transcriptional variants of p85α. 48–72 h post-transfection, cells were stimulated with EGF, insulin, platelet-derived growth factor (PDGF), or fetal bovine serum (FBS) for different time intervals before being harvested. Phospho-Akt and p85α levels were analyzed by western blot (WB) using antibodies specific for phospho-Akt and p85α. The data represent the mean ± SD from three

independent experiments. The indicated *p* value is for the 5 min time point for p85α siRNA- vs. control siRNA-treated cells.

(E) Three individual siRNAs targeting p85α show similar effects in inducing EGF-stimulated Akt activation. MDA-MB-231 cells were transfected with control siRNAs or one of three individual siRNAs targeting endogenous p85α. 48–72 h post-transfection, cells were stimulated with EGF for 5 min before being harvested. Phospho-Akt and p85α levels were analyzed by WB. The data represent the mean ± SD from three independent experiments. The indicated *p* value is for control individual p85α siRNA- vs. control siRNA-treated cells.

(F) The extent of p85α KD correlates inversely with increased EGF-stimulated Akt activation. MDA-MB-231 cells were transfected with control siRNAs or different amounts of siRNAs targeting endogenous p85α. 48–72 h post-transfection, cells were stimulated with EGF for 5 min before being harvested. Phospho-Akt and p85α levels were analyzed by WB. The data represent the mean ± SD from three independent experiments.

(G) Ectopic expression of p85α does not impair EGF-stimulated Akt activation. Cos-7 cells were transiently transfected with empty plasmid or plasmid containing p85α (FLAG-tagged p85α). 48–72 h post-transfection, cells were stimulated with EGF for different time intervals before being harvested. Phospho-Akt and p85α levels were analyzed by WB. The data represent the mean ± SD from three independent experiments. The indicated *p* value is for the 5 min time point for p85α- vs. mock-transfected cells.

(H) Ectopically expressed p85α associates with the endogenous p110α catalytic subunit. Cos-7 cells were transfected with empty plasmid or plasmid containing p85α (FLAG-tagged p85α). 48 h post-transfection, cells were harvested for immunoprecipitation (IP) of ectopically expressed p85α using anti-FLAG antibody agarose beads. Endogenous p110α that coIPed with ectopically expressed p85α was examined by WB using a p110α-specific antibody.

(I) p85α KD increases EGF-stimulated Akt activation in PTEN-null cells. PC-3 cells were transfected with control siRNAs or siRNAs targeting p85α. 48–72 h post-transfection, cells were stimulated with EGF before harvesting to examine the phospho-Akt and p85α levels by WB. The data represent the mean ± SD from three independent experiments. The indicated *p* value is for the 5 min time point for p85α siRNA- vs. control siRNA-treated cells.

(J and K) Simultaneous KD of p85α and PTEN enhances EGF-stimulated Akt activation. MDA-MB-231 cells were transfected with control siRNAs or siRNAs targeting endogenous p85α and/or PTEN. 48–72 h post-transfection, cells were either unstimulated (J) or stimulated with EGF (K) for 5 min before cell harvesting. Phospho-Akt and p85α levels were analyzed by WB using antibodies specific for phospho-Akt and p85α. The data represent the mean ± SD from three independent experiments. The indicated *p* value is for p85α KD vs. combined p85α and PTEN KD.

See also Figure S1.

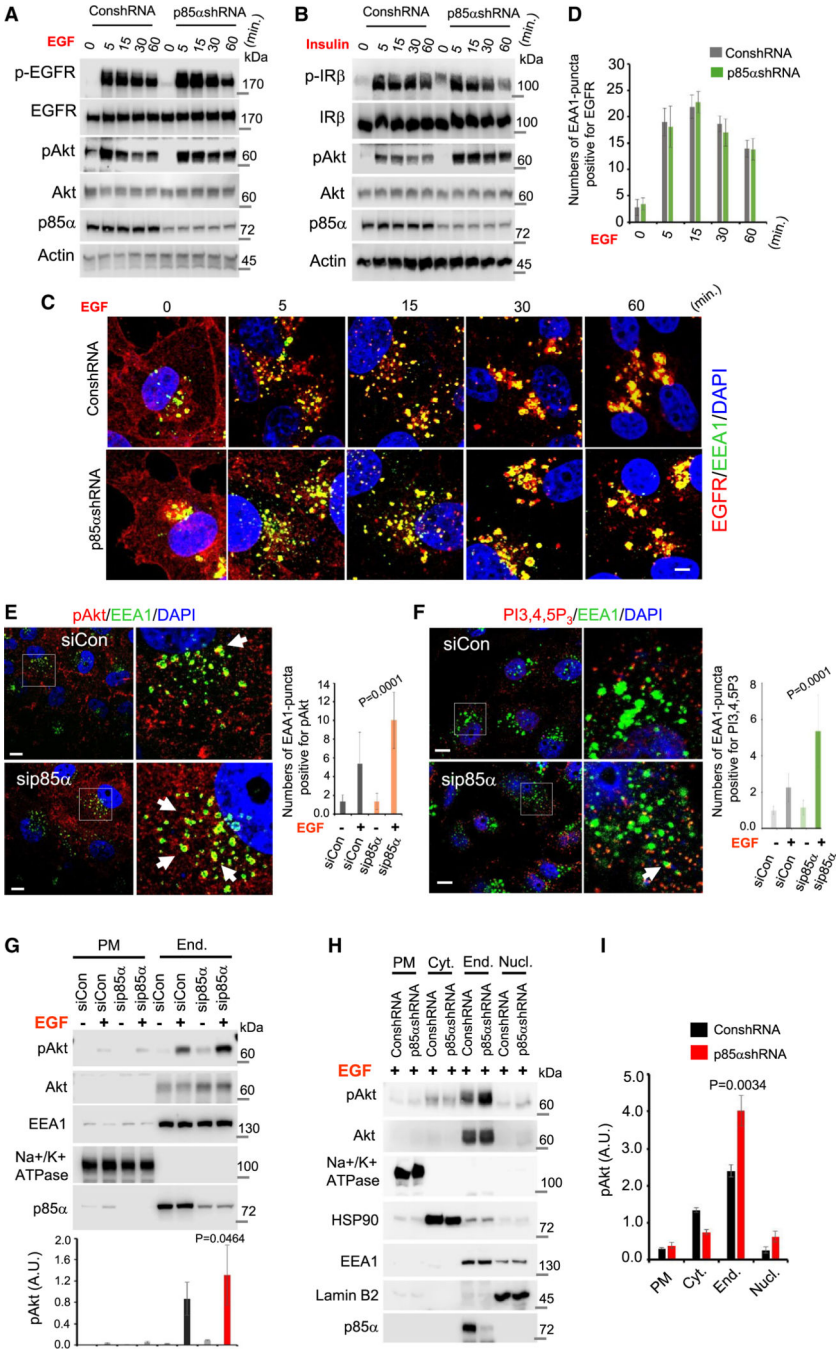

Figure 2. Agonist-stimulated PI3K/Akt signaling in response to p85α KD occurs at endosomal membranes

(A and B) Phosphorylation level of EGFR and IR at different time points following agonist stimulation. MDA-MB-231 cells with stable p85α KD were stimulated with EGF or insulin for different amounts of time before harvesting cells to examine the phosphorylation level of EGFR, IR, and Akt by WB. Representative images of three independent experiments are shown.

(C and D) Co-localization of the internalized EGFR with the endosomal marker EEA1 following EGF stimulation. MDA-MB-231 cells with stable p85α KD were stimulated with

EGF for different amounts of time before fixing the cells with 4% paraformaldehyde (PFA). The cells were immunostained with antibodies for EGFR (red) and EEA1 (green). The number of EEA1-positive puncta that were also EGFR positive was counted in at least 20–30 cells. The *p* value indicates p85α KD compared with control siRNA upon EGF stimulation. Scale bar: 10 μM.

(E and F) Activated Akt and $PI3,4,5P_3$ co-localize with endosomal marker EEA1. MDA-MB-231 cells were transfected with control siRNAs or siRNAs targeting p85α. 48–72 h post-transfection, cells were stimulated with EGF for 5 min before cell fixation with 4% PFA for IF using antibodies specific for phospho-Akt (red) or $PI3,4,5P_3$ (red) and endosomal markers EEA1 (green). The number of EEA1 puncta positive for Akt or $PI3,4,5P_3$ was counted in at least 20–30 cells. The *p* value indicates p85α KD compared with control siRNA upon EGF stimulation. Scale bar: 10 μM.

(G) Subcellular fractionation shows enrichment of activated Akt at endosomal fractions in EGF-stimulated cells. MDA-MB-231 cells were transfected with either control siRNAs or siRNAs targeting p85α. 48–72 h post-transfection, cells were stimulated with EGF for 5 min before being harvested for subcellular fractionation. Phospho-Akt levels were analyzed in the plasma membrane vs. endosomal fractions by WB. The data represent the mean ± SD from three independent experiments. The *p* value indicates p85α KD compared with control siRNA upon EGF stimulation.

(H and I) Examination of activated Akt in different subcellular fractions after EGF stimulation. A431 cells with stable p85α KD were stimulated with EGF for 5 min before being harvested for subcellular fractionation. pAkt levels were analyzed in the plasma membrane (PM), cytosol (Cyt.), endosome (End.), and nuclear (Nucl.) fractions by WB. pAkt levels in different subcellular fractions were quantified and represent the mean ± SD from three independent experiments. The *p* value indicates p85α KD compared with control. See also Figure S2.

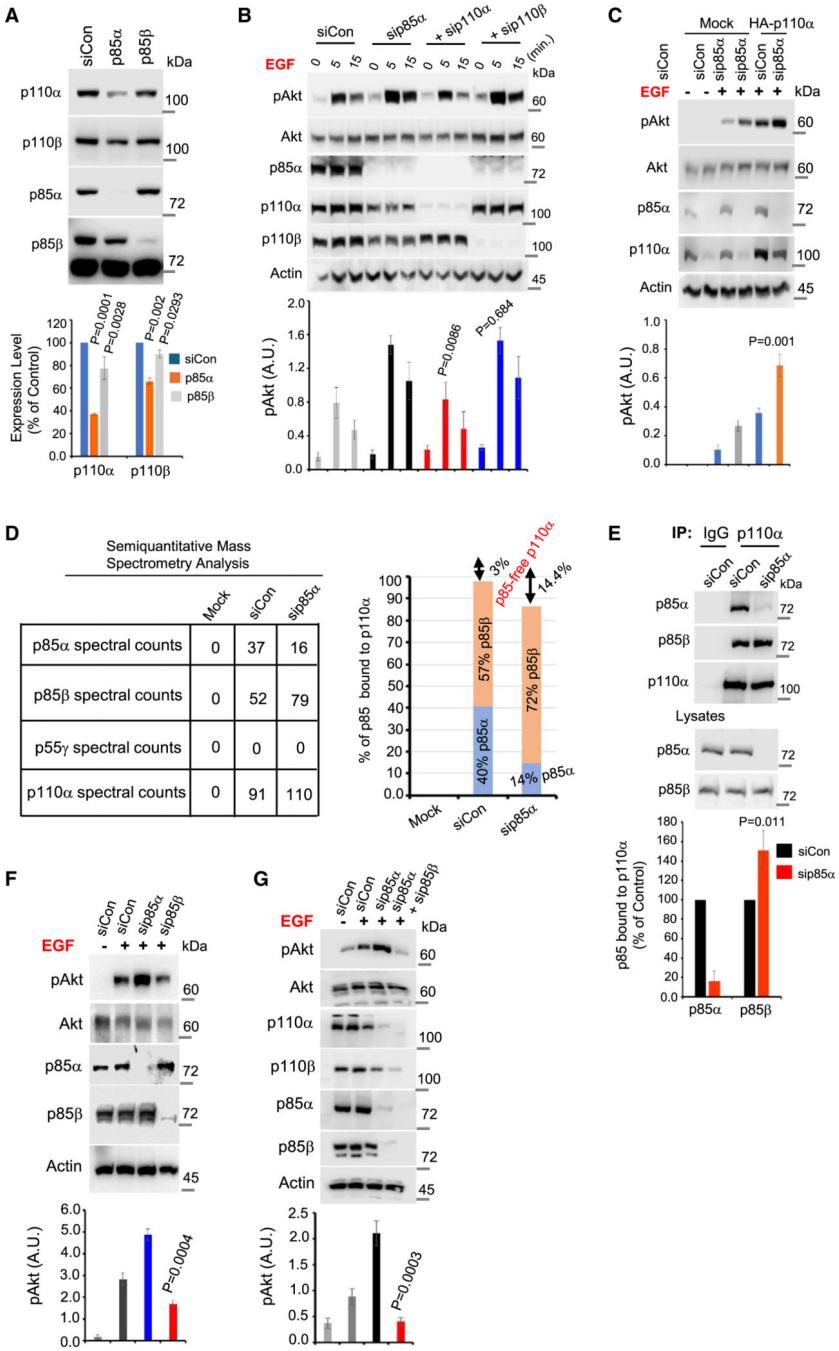

Figure 3. Residual p110α catalytic subunit is responsible for increased agonist-stimulated Akt activation upon p85α KD

(A) p85α KD decreases p110α catalytic subunit levels. MDA-MB-231 cells were transfected with control siRNAs or siRNAs targeting p85α or p85β. 48–72 h post-transfection, cells were harvested, and the expression levels of p85α, p85β, p110α, and p110β were examined by WB. The data represent the mean ± SD from three independent experiments.

(B) Residual p110α catalytic subunit is responsible for EGF-stimulated Akt activation upon p85α KD. MDA-MB-231 cells were transfected with control siRNAs or siRNAs targeting

p85α and p110α or p110β. 48–72 h post-transfection, cells were stimulated with EGF for different time intervals before being harvested. Phospho-Akt, p85α, p110α, and p110β levels were analyzed by WB. The data represent the mean ± SD from three independent experiments. The significance is indicated by *p* values (sip85α vs. sip85α/sip110α; sip85α vs. sip85α/sip110β).

(C) p85α KD promotes EGF-stimulated Akt activation in p110α-overexpressing cells. MDA-MB-231 cells stably overexpressing mock or HA-p110α-overexpressing cells were transfected with control siRNAs or siRNAs targeting endogenous p85α. 48–72 h post-transfection, cells were stimulated with EGF for 5 min before being harvested. pAkt and p85α levels were analyzed by WB. The data represent the mean ± SD from three independent experiments. The statistical significance is indicated by *p* value (sip85α in mock vs. p110α-overexpressing cells upon EGF stimulation).

(D) Mass spectrometry analysis of p110α-associated adaptor proteins. MDA-MB-231 cells stably expressing HA-p110α were transfected with control siRNAs or siRNAs targeting p85α. 48–72 h post-transfection, cells were stimulated with EGF for 5 min before being harvested. p110α was IPed using anti-HA agarose beads and coIPed proteins analyzed by mass spectrometry. The data table shows the spectral counts of IPed p110α catalytic subunit and its associated adaptor subunits and represents three independent mass spectrometry analyses.

(E) Increased association of p85β adaptor protein with p110α upon p85α KD. MDA-MB-231 cells were transfected with control siRNAs or p85α siRNAs. 48–72 h post-transfection, p110α was IPed and coIPed p85 adaptor proteins were examined by WB. The data represent the mean ± SD from three independent experiments.

(F) p85β KD impairs EGF-stimulated Akt activation. MDA-MB-231 cells were transfected with control siRNAs or siRNAs targeting p85α or p85β. 48–72 h post-transfection, cells were stimulated with EGF for 5 min before being harvested. pAkt, p85α, and p85β were analyzed by WB. The data represent the mean ± SD from three independent experiments. The statistical significance is indicated by *p* value (siCon vs. sip85β).

(G) Combined KD of p85α and p85β adaptor subunit abolishes EGF-stimulated Akt activation. MDA-MB-231 cells were transfected with control siRNAs or siRNAs targeting p85α and/or p85β. 48–72 h post-transfection, cells were stimulated with EGF for 5 min before being harvested. Phospho-Akt p85α, p85β, p110α, and p110β levels were analyzed by WB. The data represent the mean ± SD from three independent experiments. The statistical significance is indicated by *p* value (p85α siRNA vs. sip85α/sip85β).

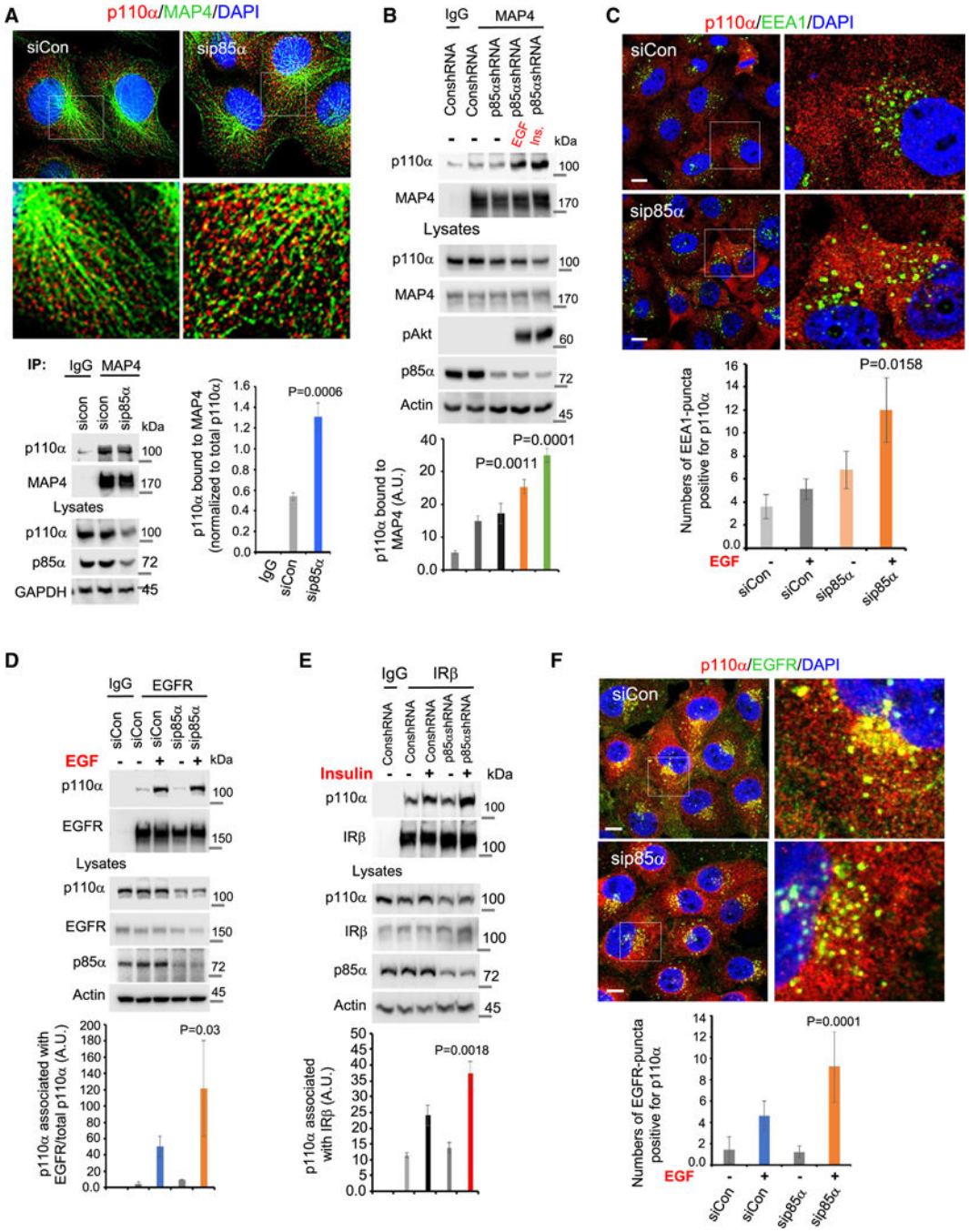

Figure 4. Residual p110α distribution along microtubules, integration into endosomal membranes, and association with agonist-stimulated receptor tyrosine kinases are enhanced upon p85α KD

(A) Residual p110α localizes along microtubules and associates with MAP4 upon p85α KD. Top, MDA-MB-231 cells were transfected with control siRNAs or siRNAs targeting p85α. 48–72 h post-transfection, cells were fixed with 4% PFA. The distribution of p110α along microtubules in cells treated with control and p85α siRNAs was examined by IF using antibodies specific for p110α (red) and MAP4 (green). Bottom, the enhanced association of residual p110α with MAP4 upon p85α KD is shown by coIP and WB. The data represent

the mean ± SD from three independent experiments. The statistical significance is indicated by *p* value (siCon vs. p85α siRNA).

(B) Agonist stimulation promotes residual p110α association with MAP4 in p85α shRNA cells. MDA-MB-231 cells with stable p85α KD were either serum starved or stimulated with EGF or insulin before being harvested. MAP4 was IPed, and the coIPed residual p110α in p85α shRNA cells was examined by WB. The data represent the mean ± SD from three independent experiments. The statistical significance is indicated by *p* value (unstimulated vs. stimulated condition in p85α shRNA cells).

(C) p110α co-localizes with endosomal markers upon p85α KD. MDA-MB-231 cells were transfected with control siRNAs or siRNAs targeting p85α. 48–72 h post-transfection, cells were stimulated with EGF and fixed with 4% PFA. The co-localization of p110α with endosomal markers in cells treated with control and p85α siRNAs was examined by IF using antibodies specific for p110α (red) and EEA1 (green). The number of EEA1-puncta positive for p110α was counted in at least 20–30 cells. The statistical significance is indicated by *p* value (control vs. p85α KD, EGF stimulated). Scale bar: 5 μM.

(D) EGF-stimulated p110α association with EGFR upon p85α KD. MDA-MB-231 cells were transfected with control siRNAs or siRNAs targeting p85α. 48–72 h post-transfection, cells were stimulated with EGF before being harvested. EGFR was IPed using anti-EGFR antibody beads, and coIPed p110α was examined by WB. The data represent the mean ± SD from three independent experiments. The statistical significance is indicated by *p* value (siCon vs. p85α siRNA, EGF stimulated).

(E) Insulin-stimulated p110α association with IRβ upon p85α KD. MDA-MB-231 cells with stable p85α KD were either serum starved or stimulated with insulin before being harvested. IRβ was IPed using anti-IRβ antibody beads, and the coIPed p110α was examined by WB. The data represent the mean ± SD from three independent experiments. The statistical significance is indicated by *p* value (unstimulated vs. insulin-stimulated p85α KD cells).

(F) EGF-stimulated p110α co-localization with EGFR upon p85α KD. MDA-MB-231 cells were transfected with control siRNAs or siRNAs targeting p85α. 48–72 h post-transfection, cells were stimulated with EGF for 5 min before fixation with 4% PFA. The co-localization of p110α with EGFR was examined by IF study using antibodies specific for p110α (red) and EGFR (green). EGFR puncta positive for p110α were counted in at least 20–30 cells. The statistical significance is indicated by *p* value (control vs. p85α KD, EGF stimulated). Scale bar: 5 μM.

See also Figure S3.

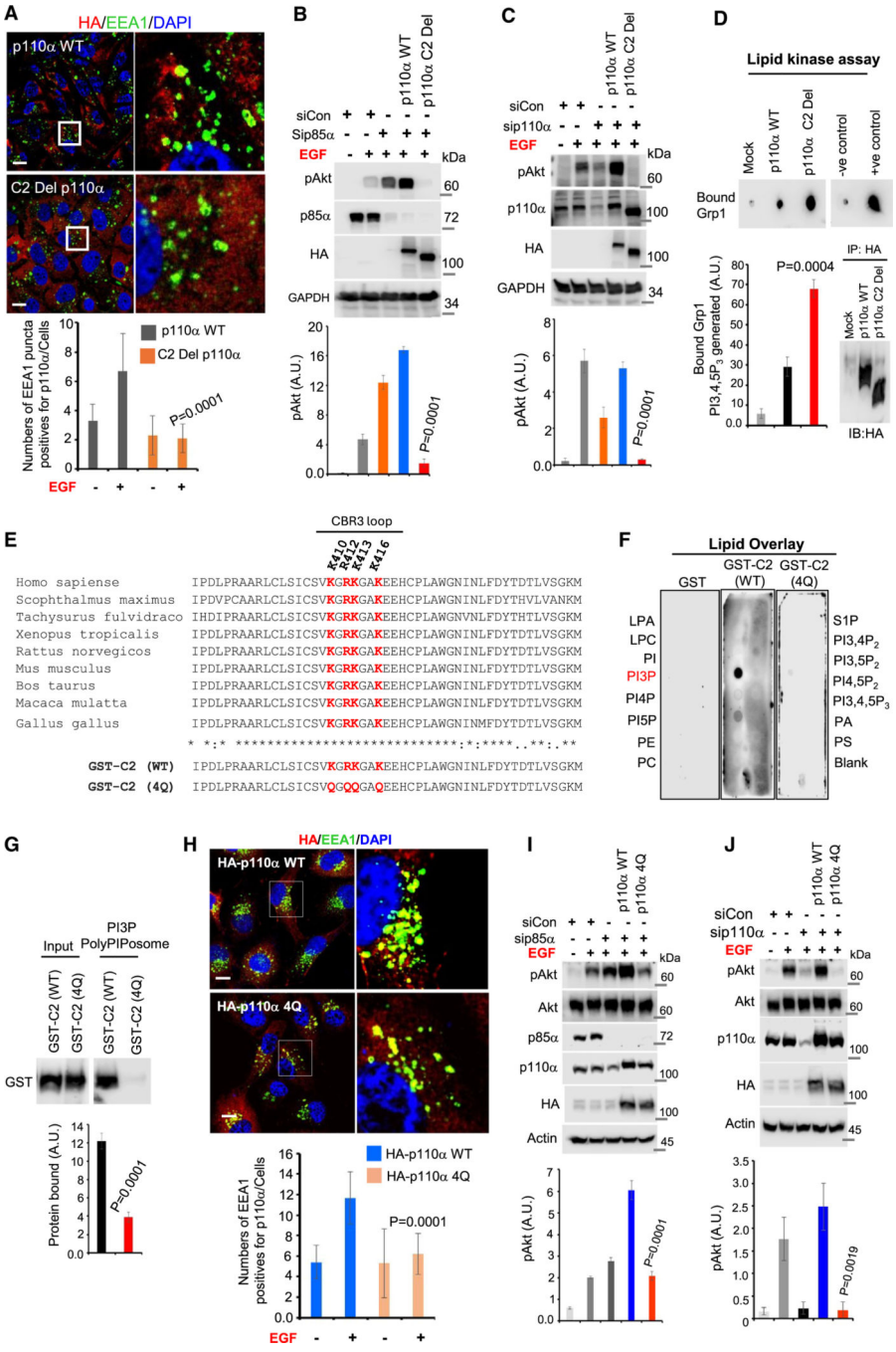

Figure 5. p110α integration into endosomes and agonist-stimulated PI3K/Akt signaling upon p85α KD are regulated by the C2 domain-PI3P interaction

(A) Deletion of p110α C2 domain impairs its integration into endosomal membranes upon agonist stimulation. MDA-MB-231 cells stably expressing wild-type (WT) HA-p110α or C2 domain deletion HA-p110α were transfected with control siRNAs or siRNAs targeting endogenous p85α. 48–72 h post-transfection, cells were stimulated with EGF for 5 min before fixation with 4% PFA. The cells were immunostained with antibodies for HA (red) and EEA1 (green). EEA1 puncta positive for HA were counted in least 20–30 cells. The

statistical significance is indicated by *p* value (control vs. p85α KD, EGF stimulated). Scale bar: 10 μM.

(B and C) C2 domain deletion mutant p110α disrupts EGF-stimulated Akt activation upon p85α KD. MDA-MB-231 cells stably expressing empty vector, WT HA-p110α, or C2 domain deletion HA-p110α were transfected with control siRNAs or siRNAs targeting endogenous p85α (B) or endogenous p110α at 3′ prime UTR regions (C) before EGF stimulation. Phospho-Akt, endogenous p85α, endogenous p110α, and HA-p110α (WT or C2 domain deletion mutant) were examined by WB. The data represent the mean ± SD from three independent experiments. The statistical significance is indicated by *p* value (WT p110α vs. C2 domain deletion mutant p110α, EGF stimulated).

(D) C2 domain deletion does not affect the *in vitro* kinase activity of p110α. p110α was immuno-isolated from MDA-MB-231 cells stably expressing WT HA-p110α or C2 domain deletion HA-p110α using anti-HA antibody agarose beads. The *in vitro* kinase activity of immuno-isolated p110α was examined using $PI4,5P_2$ micelles. The $PI3,4,5P_3$ generated in the reaction mixture was quantified by dot blot assay using GRP1-PH protein. The immuno-isolated p110α was then examined by WB. The same reaction mixture with or without purified PI3Kα holoenzyme was used as negative and positive controls for $PI3,4,5P_3$ generation. The data are the mean ± SD from at least three independent experiments. The statistical significance is indicated by *p* value (WT HA-p110α vs. C2 domain deletion mutant HA-p110α).

(E) Alignment of the p110α C2 domain from different species. The conserved lysine and arginine residues in the CBR3 loop are indicated in red. Bottom, all three lysine and one arginine residues were mutated to glutamine (4Q) to generate the mutant glutathione S-transferase (GST)-fusion protein of the C2 domain.

(F) Lipid overlay assay. The lipid overlay assay was performed by incubating the PIP-Strip membrane with purified GST-fusion proteins (each 0.5 μg/mL) overnight at 4 C°, followed by the detection of bound protein using horseradish peroxidase (HRP)-conjugated anti-GST antibody. Representative data of three independent experiments are shown.

(G) PI3P PolyPIPosome binding assay. A GST-fusion protein of the p110α C2 domain or its 4Q mutant (2 μg) was incubated with 10 μL PI3P PolyPIPosome beads. After 30 min of incubation at room temperature, the protein bound to beads was examined by WB using anti-GST antibody. The data are the mean ± SD from at least three independent experiments. The statistical significance is indicated by *p* value (WT C2 domain vs. 4Q mutant C2 domain).

(H) 4Q mutant p110α exhibits impaired integration into early endosomes. MDA-MB-231 cells stably expressing HA-p110α (WT) or C2 domain mutant p110α (4Q) were stimulated with EGF before fixing the cells with 4% PFA. The cells were immunostained with antibodies for HA (red) and EEA1 (green). EEA1 puncta that co-stained with HA were counted in least 20–30 cells. The statistical significance is indicated by *p* value (p110α WT vs. p110α 4Q, EGF stimulated). Scale bar: 10 μM.

(I and J) 4Q mutant p110α exhibits impaired EGF-stimulated Akt activation upon p85α KD. MDA-MB-231 cells stably expressing empty vector or HA-p110α (WT of 4Q mutant) were transfected with control siRNAs, p85α siRNAs (I), or siRNAs targeting endogenous p110α at 3′ prime UTR region (J) before EGF stimulation. Phospho-Akt, endogenous p110α and p85α, and HA-p110α WT or 4Q mutant levels were examined by WB. The data represent

mean ± SD from three independent experiments. The statistical significance is indicated by *p* value (p110α WT vs. p110α 4Q, EGF stimulated).

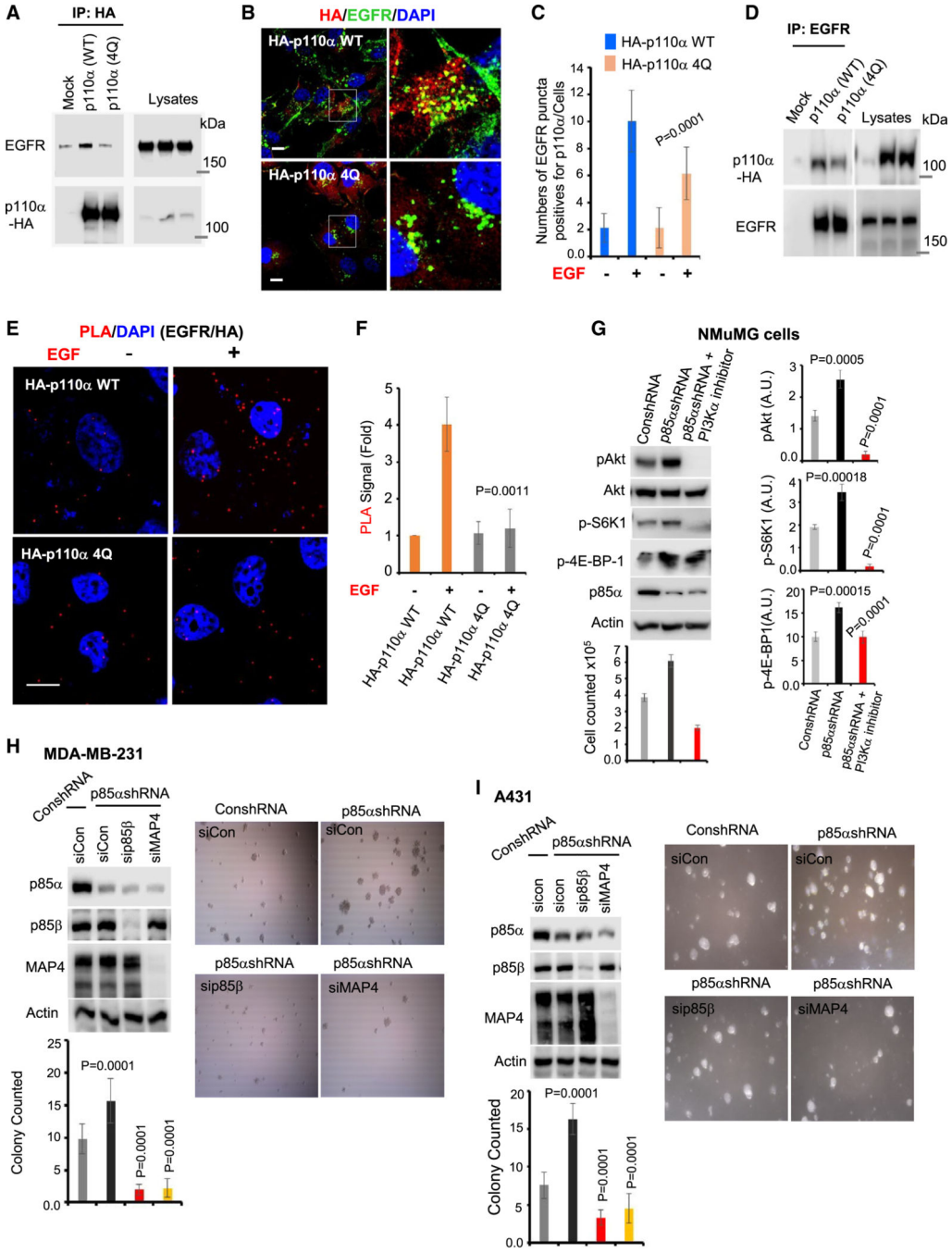

Figure 6. PI3P binding is required for p100a association with activated receptors, and tumorsphere formation mediated by p85α KD depends on p85β and MAP4

(A) Impaired association of the p110α 4Q mutant with EGFR. MDA-MB-231 cells stably expressing HA-tagged WT p110α or 4Q mutant p110α were stimulated with EGF for 5 min before being harvested. p110α was IPed using anti-HA antibody agarose beads, and the coIPed endogenous EGFR was examined by WB. The data are representative of three independent experiments.

(B and C) Impaired co-localization of the p110α 4Q mutant with EGFR. MDA-MB-231 cells stably expressing HA-tagged WT or 4Q mutant p110α were stimulated with EGF

for 3–5 min before fixing the cells with 4% PFA. The cells were immuno-stained with antibodies for HA (red) and EGFR (green). The EGFR puncta that co-localized with HA were counted in least 20–30 cells. The statistical significance is indicated by *p* value (p110α WT vs. 4Q mutant p110α, EGF stimulated). Scale bar: 10 μM.

(D) Impaired association of the p110α 4Q mutant with EGFR. COS-7 cells transiently expressing HA-tagged WT p110α or 4Q mutant p110α were stimulated with EGF for 5 min before being harvested. Endogenous EGFR was IPed, and the coIPed p110α was examined by WB. The data are representative of three independent experiments.

(E and F) PLA shows the impaired association of the p110α 4Q mutant with EGFR. COS-7 cells transiently expressing HA-tagged WT or 4Q mutant p110α were stimulated with EGF for 3–5 min before fixing the cells with 4% PFA. The cells were processed for PLA. The PLA puncta were counted in least 20–30 cells and normalized to control cells. The statistical significance is indicated by *p* value (p110α WT vs. p110α 4Q, EGF stimulated). Scale bar: 10 μM.

(G) Stable p85α KD enhances PI3K/Akt signaling and cell growth. A lentiviral shRNA system was used to stably KD p85α in NMuMG cells. Control or p85α KD cells were grown for 24 h in complete growth medium before harvesting to examine phosphorylation levels of Akt, S6K1, and 4E-BP-1 by WB. For cell growth analyses, equal numbers of cells (1×10^5 cells/well) were seeded and allowed to grow for 48 h before trypsinization and cell counting. The data represent mean ± SD from three independent experiments. The statistical significance is indicated by *p* value (conshRNA vs. p85αshRNA).

(H and I) p85β or MAP4 KD impairs increased tumorsphere formation mediated by p85α KD. Specific siRNAs were used to knock down p85β or MAP4 in MDA-MB-231 (H) and A431 (I) cells with stable p85α KD. 72 h post-transfection, cells were detached, and equal numbers of each cell type (1×10^4 cells/well) were suspended in complete medium with 3% Matrigel and allowed to grow for 6 days on ultra-low attachment plates. The number of tumorspheres formed by each cell type was counted. p85β or MAP4 KD was examined by WB. The data represent mean ± SD from three independent experiments. The statistical significance is indicated by *p* value (conshRNA vs. p85αshRNA; p85αshRNA vs. p85αshRNA with sip85β or siMAP4).

KEY RESOURCES TABLE

REAGENT or RESOURCE	SOURCE	IDENTIFIER
Antibodies		
p110α	Cell Signaling	Cat#4249; RRID:AB_2165248
p110α	Abcam	Cat#ab40776; RRID:AB_777253
p110β	Cell Signaling	Cat#3011; RRID:AB_2165246
p85α	Abcam	Cat#ab191606; RRID:AB_2891324
p85β	Abcam	Cat#ab180967
p85β	R and D	Cat#MAB6777; RRID:AB_10890218
Akt	Abcam	Cat#ab126811; RRID:AB_11128060
Akt	Cell Signaling	Cat#4298; RRID: AB_10693940
Phospho-Akt T308	Cell Signaling	Cat#2965; RRID:AB_2255933
Phospho-Akt S473	Cell Signaling	Cat#4060; RRID:AB_2315049
Phospho-Akt	Invitrogen Life Technologies	Cat#OMA1–03061
PI3,4,5P3	Echelon Biosciences	Cat#Z-P345; RRID:AB_427226
MAP4	Santa Cruz Biotechnologies	Cat#sc-390286
MAP4 agarose beads	Santa Cruz Biotechnologies	Cat#sc-390286AC
Normal mouse IgG beads	Santa Cruz Biotechnologies	Cat#sc-2343AC
HA	Cell Signaling	Cat#3724; RRID: AB_1549585
HA agarose beads	ThermoFisher Scientific	Cat#26181
FLAG	Cell Signaling	Cat#2368; RRID:AB_2217020
FLAG M2 Affinity Gel	Sigma-Aldrich	Cat#F2426; RRID:AB_2616449
GST-HRP	Amersham	Cat#RPN1236V
GAPDH	Cell Signaling	Cat#2118; AB_561053
Tubulin	Abcam	Cat#18251; RRID: AB_2210057
EEA1	BD Biosciences	Cat#610457; RRID:AB_397830
EEA1	Cell Signaling	Cat#3288; RRID:AB_2096811
TFR	Invitrogen	Cat#136800; RRID:
TFR	Abcam	Cat#ab84036; RRID:AB_10673794
Normal rabbit IgG beads	Cell Signaling	Cat#2729; RRID:AB_1031062
Rabbit anti-EGFR beads	Cell Signaling	Cat#5735; RRID:AB_10691854

REAGENT or RESOURCE	SOURCE	IDENTIFIER
EGFR	Santa Cruz Biotechnologies	Cat#sc-120
Phospho-EGFR	Cell Signaling	Cat#2234; RRID:AB_331701
Actin	Cell Signaling	Cat#4967; RRID:AB_330288
PTEN	Santa Cruz Biotechnologies	Cat#7974
Phospho-mTOR	Cell Signaling	Cat#2971; RRID:AB_330970
Phospho-PDK1	Proteintech	Cat#29241–1-AP; RRID:AB_2918256
Phospho-S6K1	Cell Signaling	Cat#9205; RRID:AB_330944
Phospho-4EBP1	Cell Signaling	Cat#9459; RRID:AB_330985
Phospho-IRβ	Santa Crutz Biotechnologies	Cat#sc-81500
Na+/K + ATPase	Cell Signaling	Cat#3010; RRID:AB_2060983
IRβ	Santa Cruz Biotechnologies	Cat#sc-711
IRα agarose beads	Santa Cruz Biotechnologies	Cat#sc-57344AC
HRP Goat anti-rabbit IgG (H + L)	Jackson ImmunoResearch	Cat#111–035-144; RRID:AB_2307391
HRP Goat anti-mouse IgG (H + L)	Jackson ImmunoResearch	Cat#115–035-166; AB_2338511
Bacterial and virus strains		
DH5α	Invitrogen	Cat#18–258-012
BL21	ThermoFisher Scientific	Cat#EC0114
STBL3	Invitrogen	Cat#C7373–03
Chemicals, peptides, and recombinant proteins		
PI(3,4,5)P3 Grip	Echelon Biosciences	Cat#G-3901
Polybrene	Santa Cruz Biotechnologies	Cat#sc-134220
Calcium phosphate transfection reagents	Sigma-Aldrich	Cat#CAPHOS
EGF	Millipore Sigma	Cat#E9644
Insulin	Millipore Sigma	Cat#I2643
PDGF	Millipore Sigma	Cat#P3201
LipofectamineTM 3000	Invitrogen	Cat#L3000001
Lipofectamine RNAiMAX	Invitrogen	Cat#13778150
PI3Kα inhibitor (Alpelisib)	Selleckchem	Cat#S2814
Critical commercial assays		

REAGENT or RESOURCE	SOURCE	IDENTIFIER
Plasmid DNA Maxiprep kit	ThermoFisher Scientific	Cat#K210016
Plasmid DNA miniprep kit	ThermoFisher Scientific	Cat#K210002
pfuUltra High-Fidelity DNA Polymerase	Agilent	Cat#600385
Endosome isolation kit	Envent Biotechnologies	Cat#ED-028
Matrigel	Corning	Cat#356231
Experimental models: Cell lines		
MDA-MB-231	ATCC	Cat#HTB-26
A431	ATCC	Cat#CRL-1555
HEK293T	ATCC	Cat#CRL-3216
HCT116	ATCC	Cat#CCL-247
NMuMG	ATCC	Cat#CRL-1636
COS-7	ATCC	Cat#CRL-1651
H4	ATCC	Cat#HTB-148
Oligonucleotides		
See method details for sequences		N/A
Recombinant DNA		
pWPT-GFP	Addgene	RRID:Addgene_12255
pMD2.G	Addgene	RRID: Addgene_12259
psPAX2	Addgene	RRID:Addgene_12260
HA-p110α (WT)	This paper	N/A
HA-p110α (C2 Del.)	This paper	N/A
HA-p110α (4Q Mutant)	This paper	N/A
Flag-p85α	Aggene	RRID:Addgene_13429